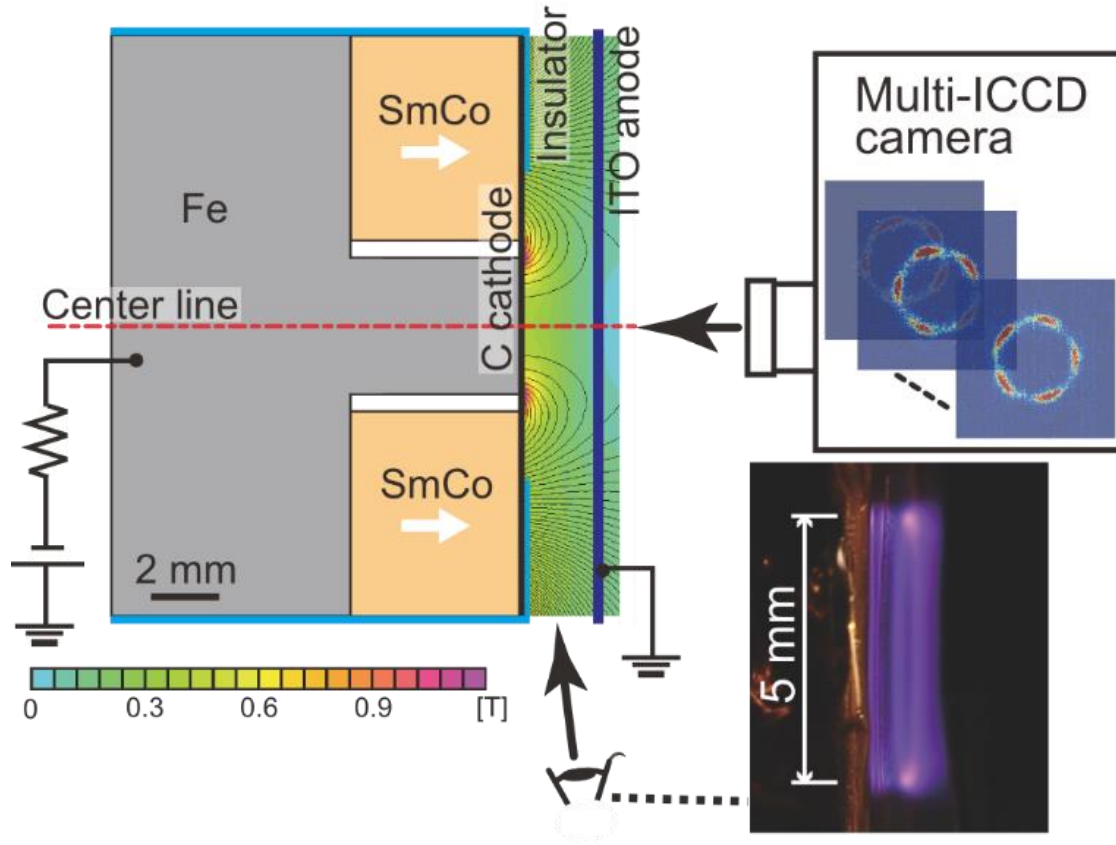


Voltage-dependent coherent drift
modes and turbulent transition
regimes in small magnetron devices

M. Cappelli

T. Ito, N. Gascon, and A. Marcovati, C. Young
Stanford University

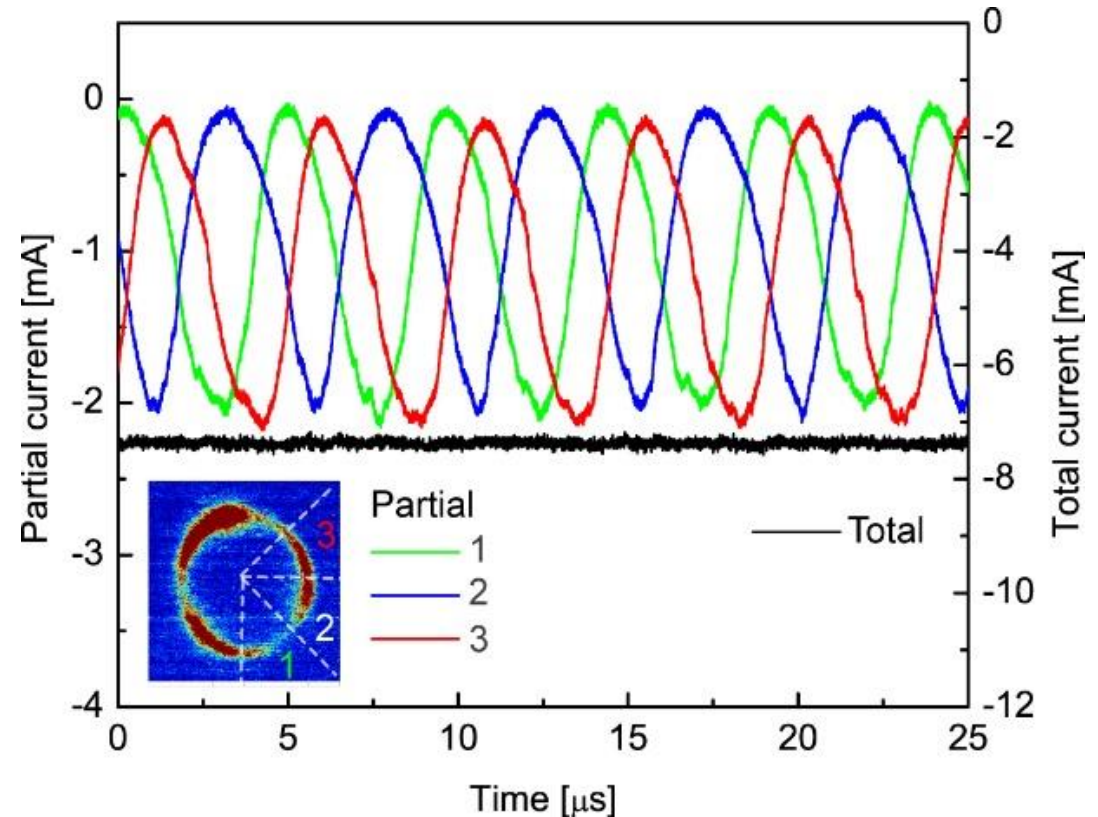
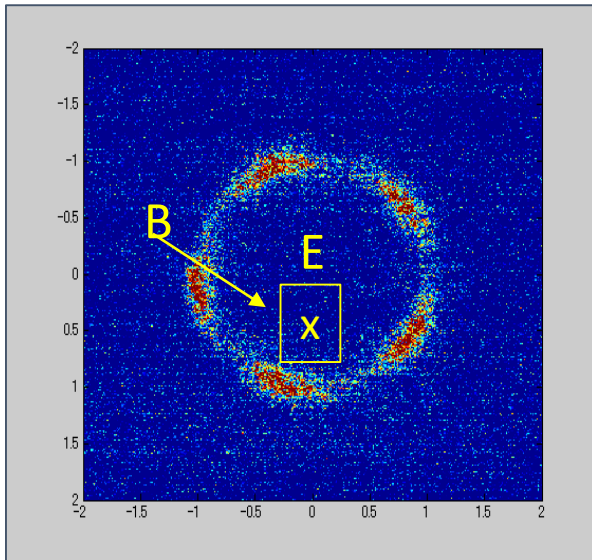
Magnetron Details



- Very small (~ 5 mm diameter discharge, 2 mm gap)
- Strong radially-inward B (~ 1 T B_{peak} , $0.3 - 5$ T B_{plasma})
- Low pressure (~ 100 mTorr)
- Very strong axial gradients (mm) – expect gradient drifts
- Indium-tin-oxide anode (transparent)

Coherent Rotating Modes

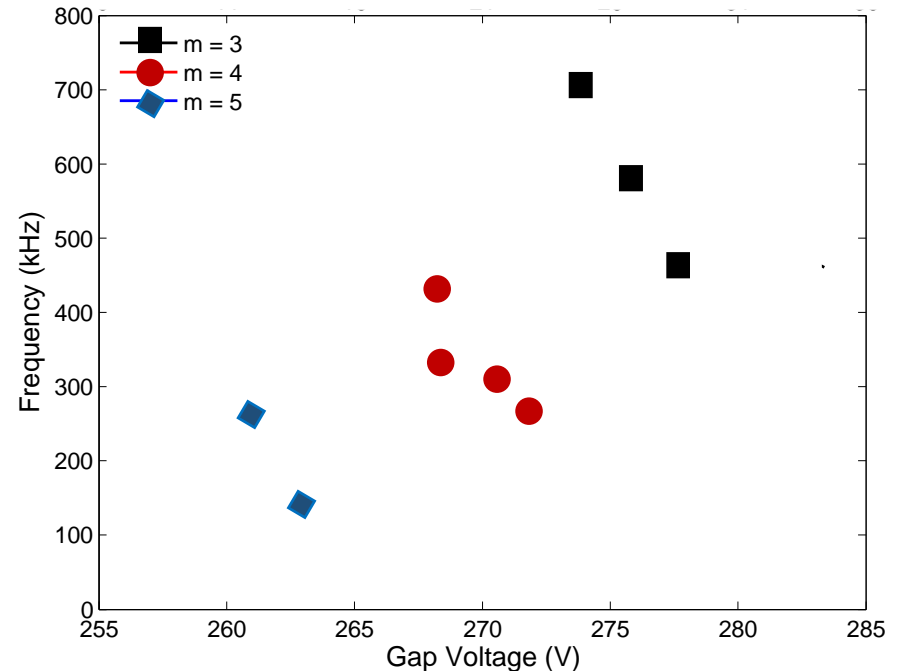
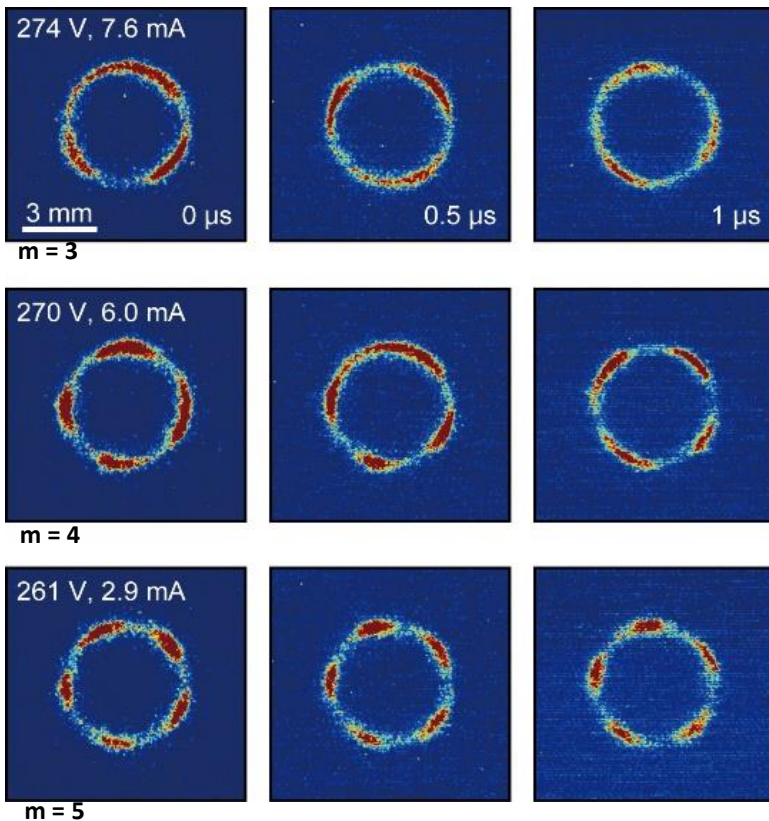
$E \times B$ is Counter Clockwise



- unambiguous direction confirmed by varying framing rate
- the structures rotate in the $-E \times B$ direction (retrograde)
- coherent (segmented anode confirms current-carrying)
- the total discharge current shows no evidence of fluctuations

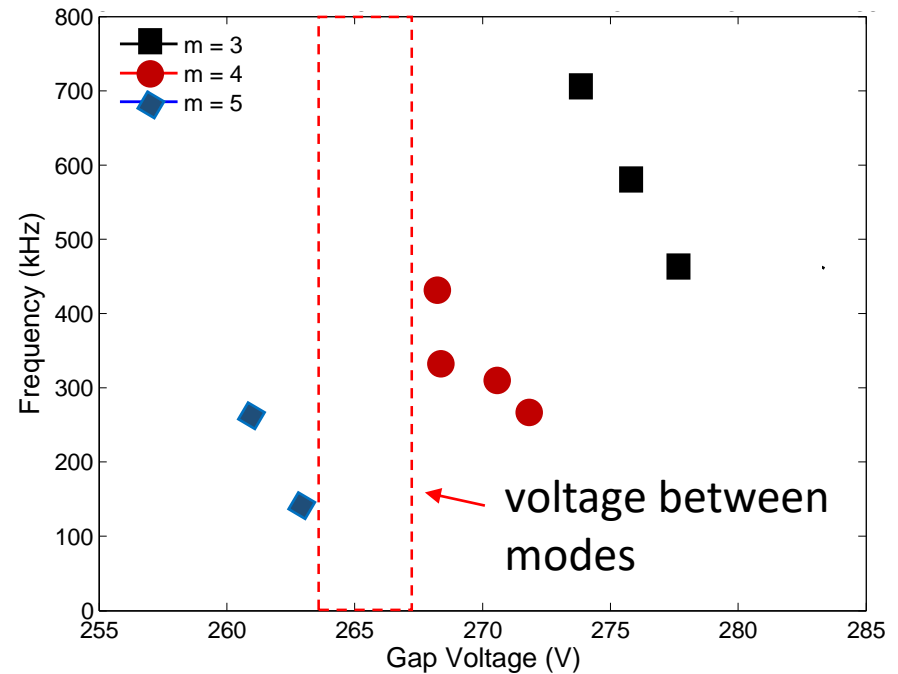
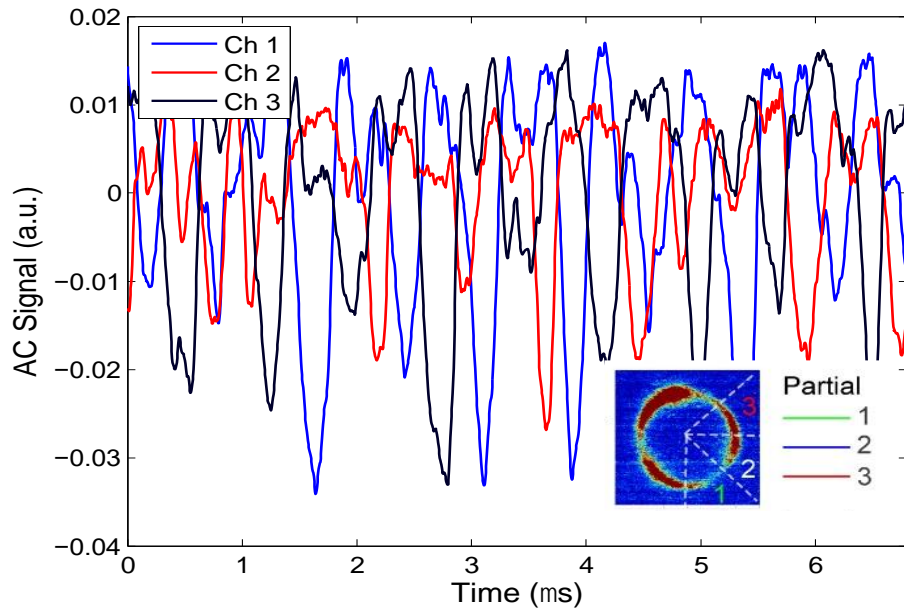
Instability Controlled by Gap Voltage

Movie frames



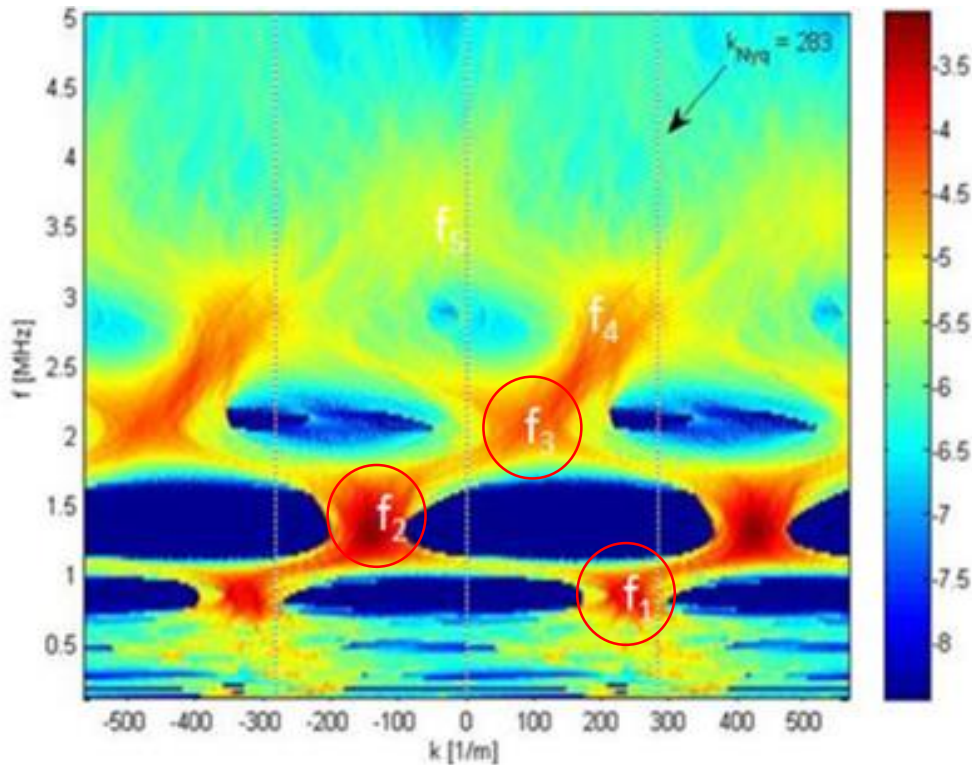
- discharge gap voltage controls structure **frequency** and **mode**
- within mode: frequency **decreases** with increasing voltage (unexpected)!
- wavelength of the modes **increase** (m decreases) with increasing voltage

“Turbulent” Regimes between Coherent States

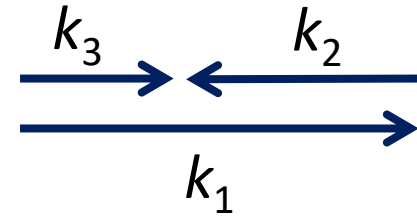


- temporal behavior of oscillations erratic/turbulent between modes
- broad range of frequencies
- anode segments serve as “probes” for wavelet analysis
- wavenumber Nyquist $\sim 280 \text{ m}^{-1}$

Three-wave coupling



3-wave mixing in azimuthal waves



$$f_1(0.85) + f_2(1.31) = f_3(2.16) \quad \text{MHz}$$

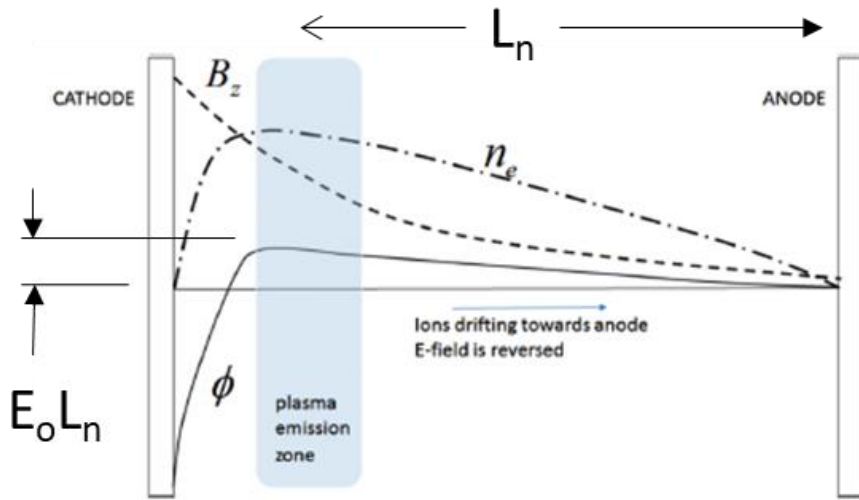
$$k_1(230) + k_2(-130) = k_3(100) \quad \text{m}^{-1}$$

$$f_2(1.31) + f_3(2.16) = f_5(3.47) \quad \text{MHz}$$

$$k_2(-130) + k_3(100) = k_5(-30) \quad \text{m}^{-1}$$

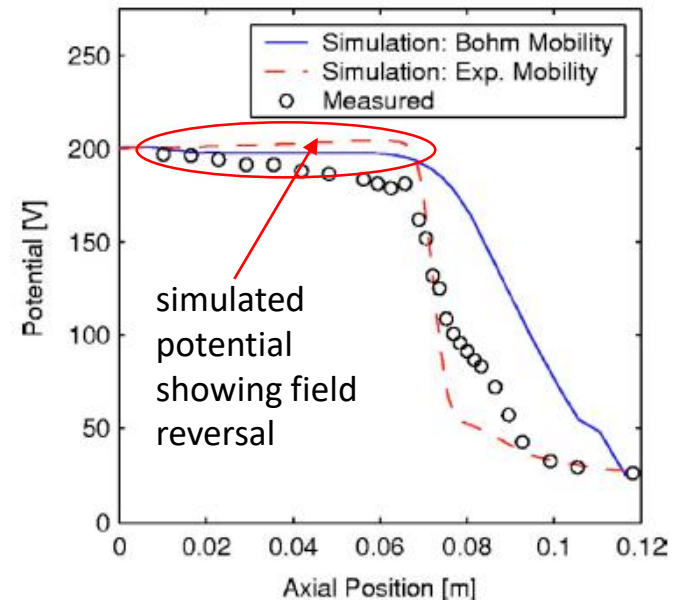
- wavelet analysis reveals high frequency quasi-coherent states (\sim five) with strong interconnectivity
- three-wave coupling satisfying momentum and energy selection rules

Hypothesis for Retrograde Motion

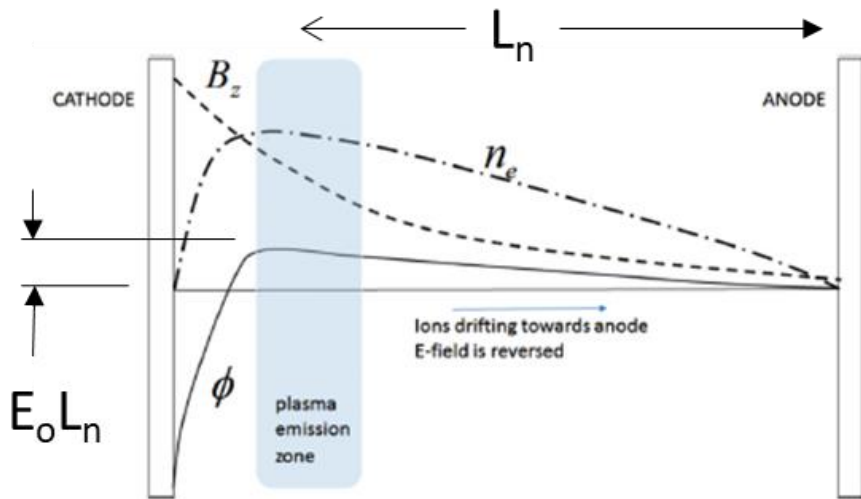


- J comparable to Hall thrusters ($\sim 0.1 \text{ A/cm}^2$)
 - similar densities/smaller length scale
- field reversal necessary to restrict diffusion-driven electrons
- plasma rotation in local $E \times B$ direction
- field drives ions towards anode

- field reversals predicted in anode region of Hall thrusters
 - potential well $\sim 5 \text{ V}$
- causes ions to stream towards anode
- region of strong ionization
- can potentially lead to reversal in ionization (S-H) spoke instabilities

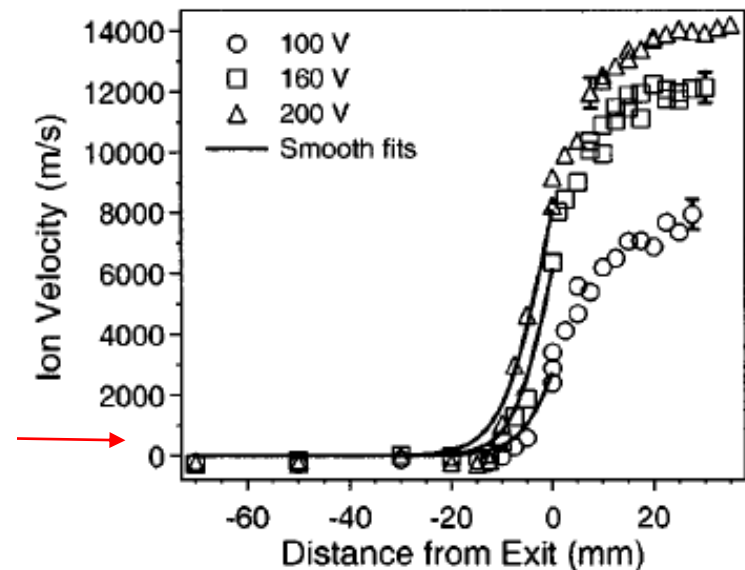


Hypothesis for Retrograde Motion



- J comparable to Hall thrusters ($\sim 0.1 \text{ A/cm}^2$)
 - similar densities/smaller length scale
- field reversal necessary to restrict diffusion-driven electrons
- plasma rotation in local $E \times B$ direction
- field drives ions towards anode

- field reversals predicted in anode region of Hall thrusters
 - potential well $\sim 5 \text{ V}$
- causes ions to stream towards anode
- region of strong ionization
- can potentially lead to reversal in ionization (S-H) spoke instabilities
- **anode-streaming ions seen in early LIF data (Meezan et al 2001)**



Meezan, et al, 2001. *Physical Review E*, 63(2), p.026410.

Gradient Drift-wave Theory

source term :
ionization and
diffusive loss along B

Governing Equations

electron mass and momentum $\frac{\partial n}{\partial t} + \mathbf{V}_{E \times B} \cdot \nabla n - 2n(\mathbf{V}_{E \times B} + \mathbf{V}_D) \cdot \nabla \ln B_0 = v_I n + D_A \frac{\partial n}{\partial z}$

ion mass $\frac{\partial n}{\partial t} + \nabla \cdot n\mathbf{v} = v_I n + D_A \frac{\partial n}{\partial z}$

ion momentum $\frac{\partial \mathbf{v}}{\partial t} + (\mathbf{v} \cdot \nabla)\mathbf{v} + \frac{q}{M} \nabla \phi = 0$

$$\mathbf{V}_{E \times B} = -\frac{\mathbf{B}_0}{B_0^2} \times \mathbf{E}$$

$$\mathbf{V}_D = -\frac{\mathbf{B}_0}{B_0^2} \times \frac{kT}{en} \nabla n$$

Linear Perturbation – Fourier Analyzed

$$\frac{\tilde{n}}{n_0} = \frac{k_{\perp}^2}{(\omega - k_x v_{ox})^2} \frac{e\tilde{\phi}}{M} \quad \tilde{v}_x = \frac{k_x}{\omega - k_x v_{ox}} \frac{e\tilde{\phi}}{M} \quad \tilde{v}_y = \frac{k_y}{\omega - k_x v_{ox}} \frac{e\tilde{\phi}}{M} \quad \text{Ions}$$

$$\frac{\tilde{n}}{n_0} = \frac{\omega^* - \omega_D}{\omega - \omega_0 - \omega_D + iv^*} \frac{e\tilde{\phi}}{kT} \quad \tilde{V}_x = -\frac{ik_y}{B_0} \tilde{\phi} = -\frac{ik_y}{B_0} \frac{kT}{en_0} \frac{\omega - \omega_0 - \omega_D + iv^*}{\omega^* - \omega_D} \tilde{n} \quad \text{Elec}$$

$$\omega^2 - \left(2k_x v_{ox} + \frac{c_s^2 k_{\perp}^2}{\omega^* - \omega_0}\right) \omega + (k_x v_{ox})^2 + \frac{c_s^2 k_{\perp}^2 (\omega_0 + \omega_D)}{\omega^* - \omega_D} - \frac{ic_s^2 k_{\perp}^2 v^*}{\omega^* - \omega_D} = 0$$

anode-streaming ion velocity
(depends on well depth $E_0 L_n$)

net loss (diffusion less ionization)
 $v^* = k_z^2 D_A - v_I$

Gradient Drift-wave Theory

source term :
ionization and
diffusive loss along B

Governing Equations

electron mass and momentum $\frac{\partial n}{\partial t} + \mathbf{V}_{E \times B} \cdot \nabla n - 2n(\mathbf{V}_{E \times B} + \mathbf{V}_D) \cdot \nabla \ln B_0 = v_I n + D_A \frac{\partial n}{\partial z}$

ion mass $\frac{\partial n}{\partial t} + \nabla \cdot n\mathbf{v} = v_I n + D_A \frac{\partial n}{\partial z}$

ion momentum $\frac{\partial \mathbf{v}}{\partial t} + (\mathbf{v} \cdot \nabla)\mathbf{v} + \frac{q}{M} \nabla \phi = 0$

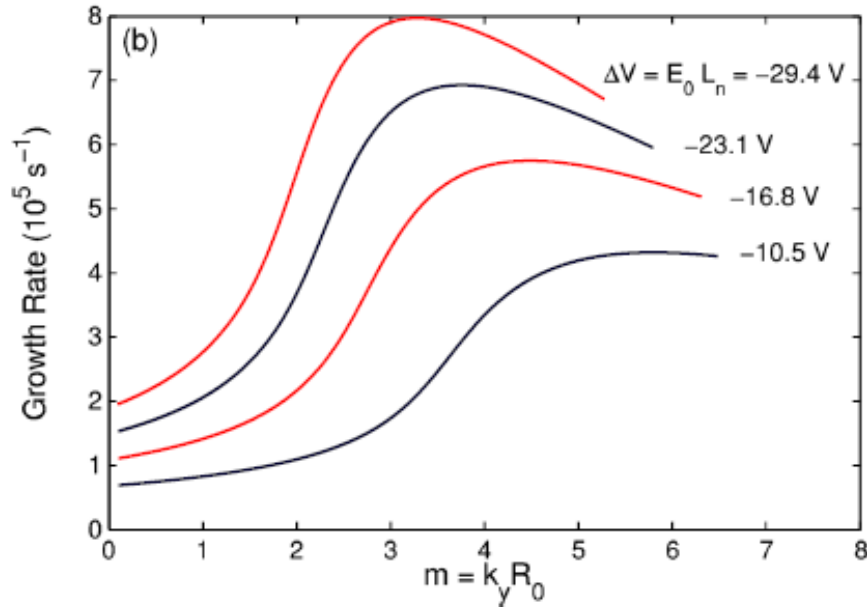
$$\mathbf{V}_{E \times B} = -\frac{\mathbf{B}_0}{B_0^2} \times \mathbf{E}$$

$$\mathbf{V}_D = -\frac{\mathbf{B}_0}{B_0^2} \times \frac{kT}{en} \nabla n$$

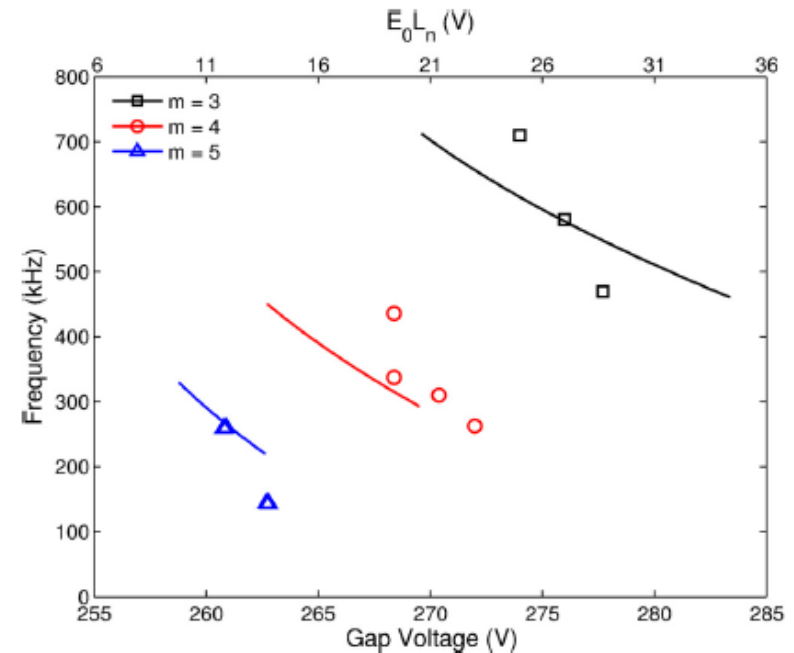
Simon-Hoh (like) Instability but the B-field curvature (drift) term overtakes the density gradient term relieving the requirement of the usual S-H condition that $E_0 \frac{dn}{dx} > 0$.

Comparison to Experiments

Growth Rate



Frequency



- peak growth rate depends on well depth (voltage)
 - increased field (voltage) favors lower mode number (as seen in experiments)
 - expect a hysteresis (also seen in experiments)
- within a mode, increasing voltage decreases frequency

Coherent Fluctuations Drive Transport

Electron Current Density

$$J_e = \text{Re}\{e\tilde{n}\tilde{V}_x\} = -\frac{k_y n_o kT}{B_o} \left(\frac{\tilde{n}}{n_o}\right)^2 \frac{v^*}{(\omega^* - \omega_D)} \approx \frac{1}{2} e n_o L_{\nabla} v^* \left(\frac{\tilde{n}}{n_o}\right)^2$$

To match the experiment frequencies

$$v^* = 3 \times 10^6 \text{ s}^{-1}$$

$$L_{\nabla} \approx 10^{-3} \text{ m}$$

If we further assume:

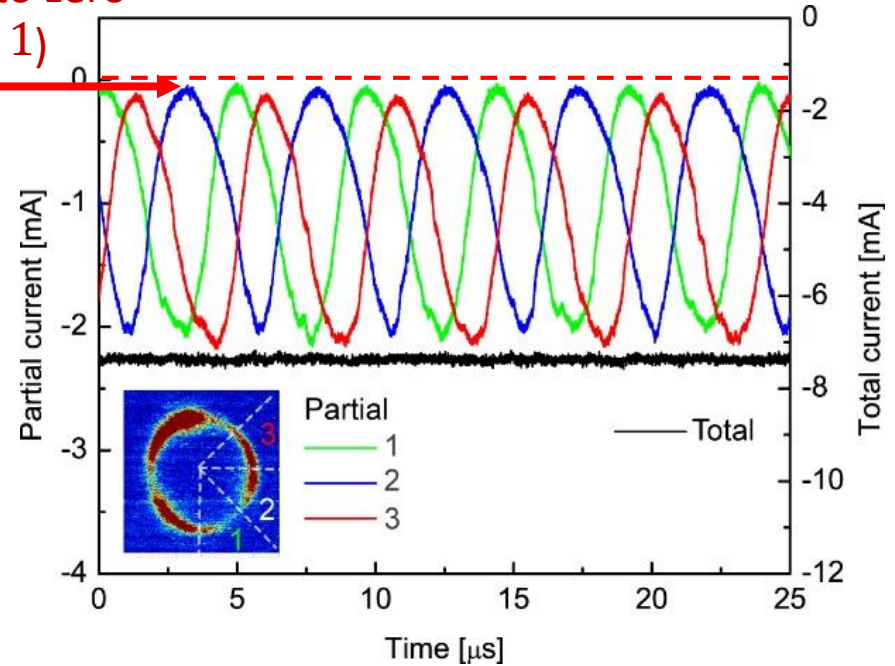
$$n_o = 10^{18} \text{ m}^{-3}$$

$$\left(\frac{\tilde{n}}{n_o}\right)^2 \approx 1$$

→ $J_e \approx 0.5 \text{ A/m}^2$

Consistent with experimental estimates of current density

Current falls to zero (so $\tilde{n}/n_o \approx 1$)



$$J_e = \text{Re}\{e\tilde{n}\tilde{V}_x\} = \text{Model}$$

$v^* = 3 \times 10^6 \text{ s}^{-1}$
 $L_{\nabla B} = 2 \times 10^{-3} \text{ m}$

Summary

- small magnetron discharge can generate very coherent plasma oscillations
- fluctuations propagate opposite external $E \times B$ direction
 - likely due to presence of field reversal (potential well) driven by strong gradients in plasma density
 - drift-wave theory describes this behavior fairly well
- “turbulence” between modes
 - evidence of three-wave coupling within this turbulence
- transport during the coherent modes consistent with drift theory
 - S-H “like” with strong curvature drift term
 - cross-field current uniquely determined by gradient length scale and ionization

Acknowledgements: AFOSR

Extra Slides

Linear Perturbation – Fourier Analyzed

$$\frac{\tilde{n}}{n_o} = \frac{\omega^* - \omega_D}{\omega - \omega_o - \omega_D + i\nu^*} \frac{e\tilde{\phi}}{kT}$$

$$\tilde{v}_x = \frac{k_x}{\omega - k_x v_{ox}} \frac{e\tilde{\phi}}{M}$$

$$\frac{\tilde{n}}{n_o} = \frac{k_{\perp}^2}{(\omega - k_x v_{ox})^2} \frac{e\tilde{\phi}}{M}$$

$$\tilde{v}_y = \frac{k_y}{\omega - k_x v_{ox}} \frac{e\tilde{\phi}}{M}$$

$$\tilde{V}_x = -\frac{ik_y}{B_o} \tilde{\phi} = -\frac{ik_y}{B_o} \frac{kT}{en_o} \frac{\omega - \omega_o - \omega_D + i\nu^*}{\omega^* - \omega_D} \tilde{n}$$

$$Re\{e\tilde{n}\tilde{V}_x\} = \frac{k_y}{B_o} \frac{kT}{en_o} \frac{\nu^*}{\omega^* - \omega_D} \left(\frac{\tilde{n}}{n_o}\right)^2$$

$$\omega^2 - \left(2k_x v_{ox} + \frac{c_s^2 k_{\perp}^2}{\omega^* - \omega_D}\right) \omega + (k_x v_{ox})^2 + \frac{c_s^2 k_{\perp}^2 (\omega_o + \omega_D)}{\omega^* - \omega_D} - \frac{ic_s^2 k_{\perp}^2 \nu^*}{\omega^* - \omega_D} = 0$$

anode-streaming ion velocity
(depends on well depth $E_o L_n$)

net source (ionization and diffusion)

Characteristics Frequencies

$$\omega^* = -\frac{c_s^2 k_y}{\omega_{ic} L_{\nabla n}}$$

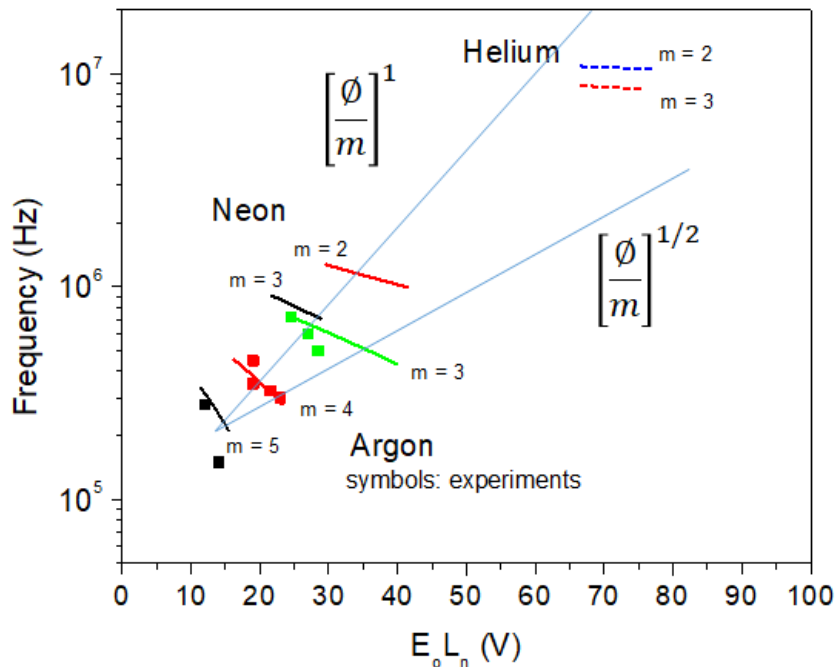
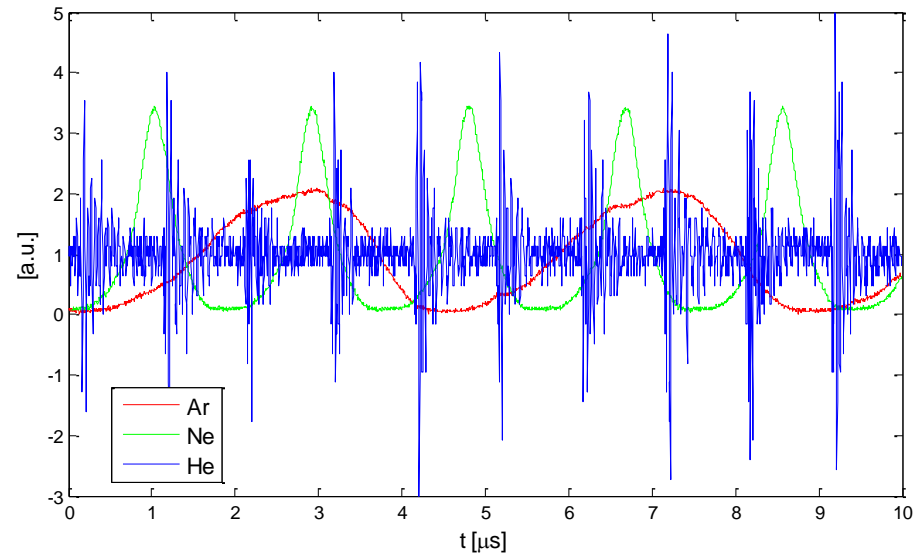
$$\omega_D = -\frac{c_s^2 k_y}{\omega_{ic} L_{\nabla B}}$$

$$\omega_o = k_y V_{E \times B}$$

Behavior shows strong dependence on ion mass

First experiments with Ne, He

- Frequency/mode increases with decreasing M!
 - Ar ($m = 3$) = 200 kHz,
 - Ne ($m = 1$) = 500 kHz
 - He ($m = 0$) = 10 MHz
- Ar (linear), Ne (non-linear), He (pulsating at ~ 0.5 -1MHz)



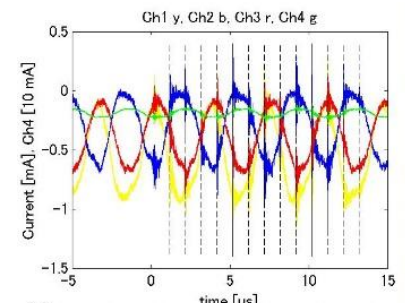
Primary scaling of frequency

- frequency of oscillations scaling:

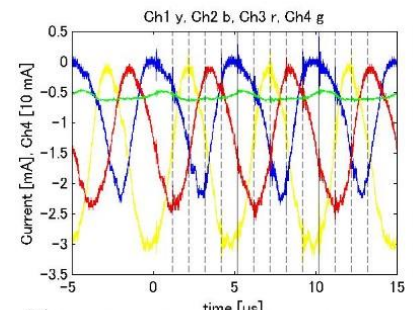
$$\left[\frac{\phi}{M}\right]^{1/2} < f < \left[\frac{\phi}{M}\right]^1$$

- Primary scaling however does not describe the inverse voltage dependence within modes

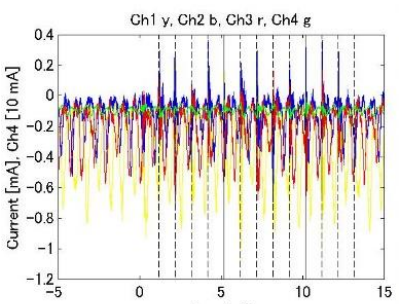
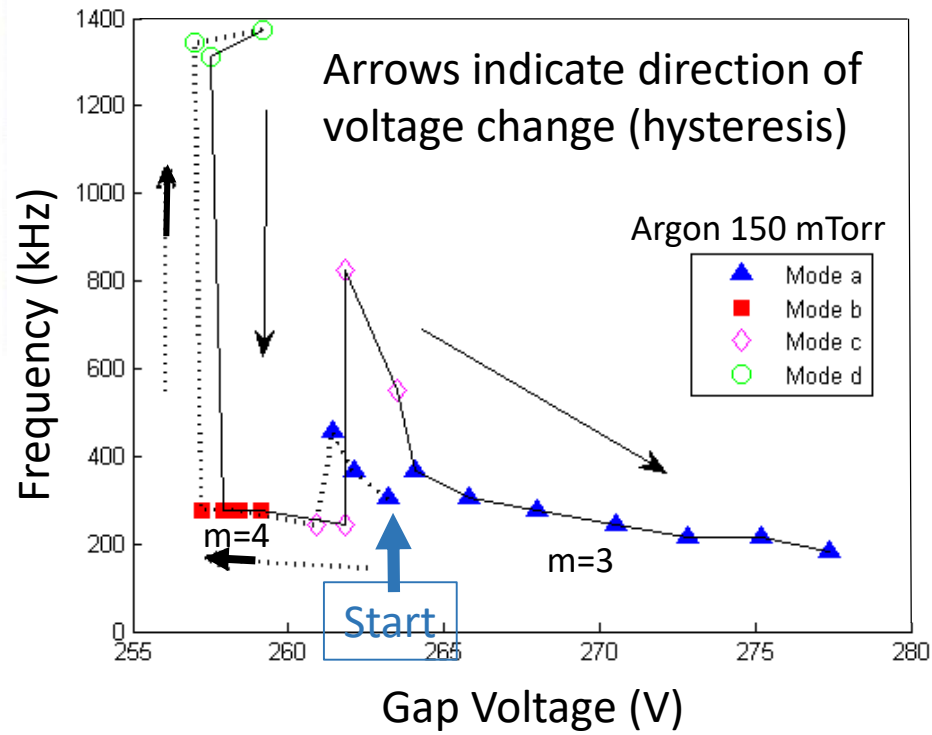
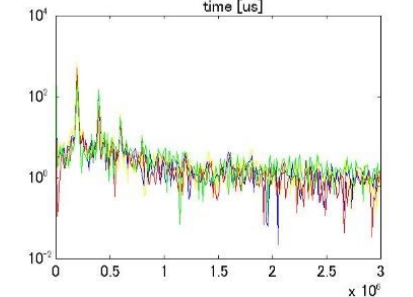
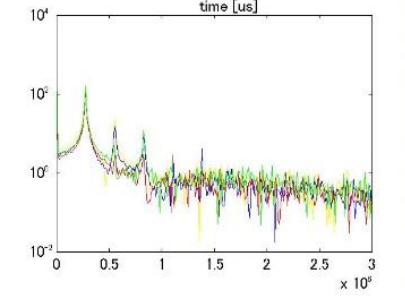
Complex regimes between azimuthal modes



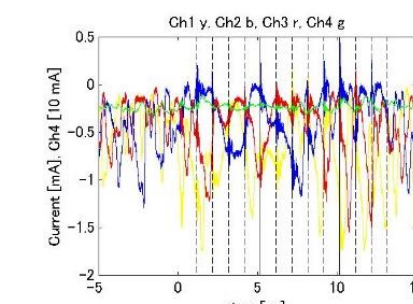
Mode b
coherent
 $m = 4$



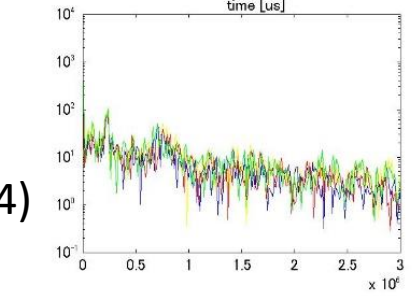
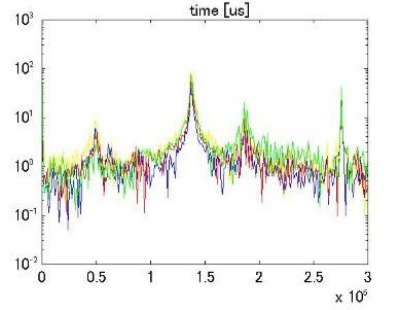
Mode a
coherent
 $m = 3$



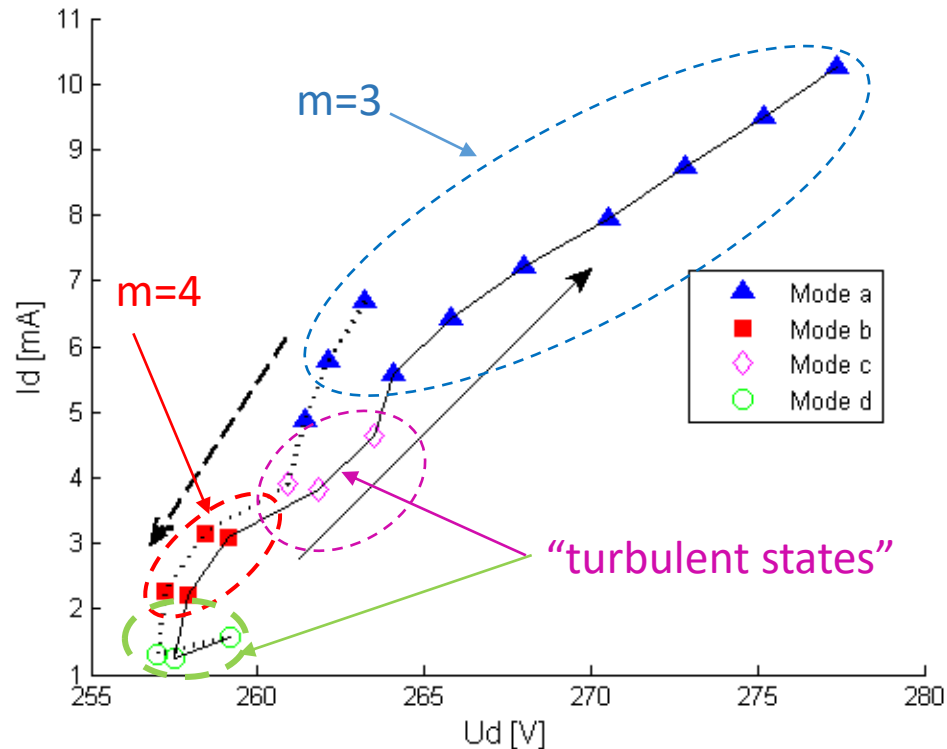
Mode d
Turbulent
(between $m = 4/5$)



Mode c
Turbulent
(between $m = 3/4$)



Transport and current flow: resistive behavior



- hysteresis in I-V curve with increasing/decreasing current
- “turbulent state” between $m = 3$, $m = 4$ modes (reproducible)
- turbulent states do not greatly enhance the current
- turbulent case near $m = 4$, $m = 5$ boundary exhibits non-linear wave-coupling

Breathing mode dynamic via time-
resolved ion velocities in a BHT-600
Hall thruster

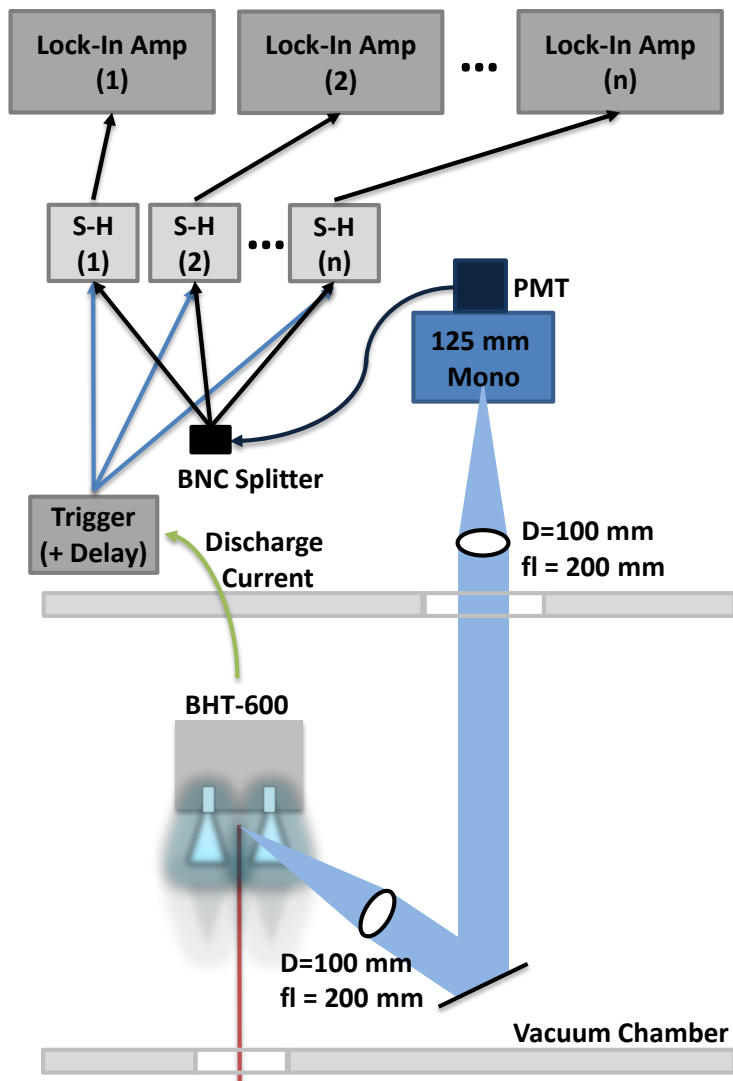
M.A. Cappelli

C.V. Young and A. Lucca-Fabris

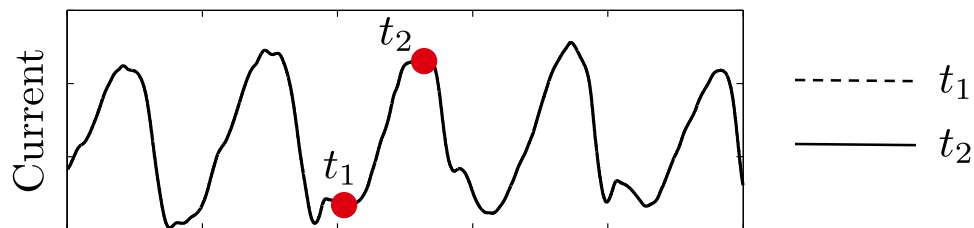
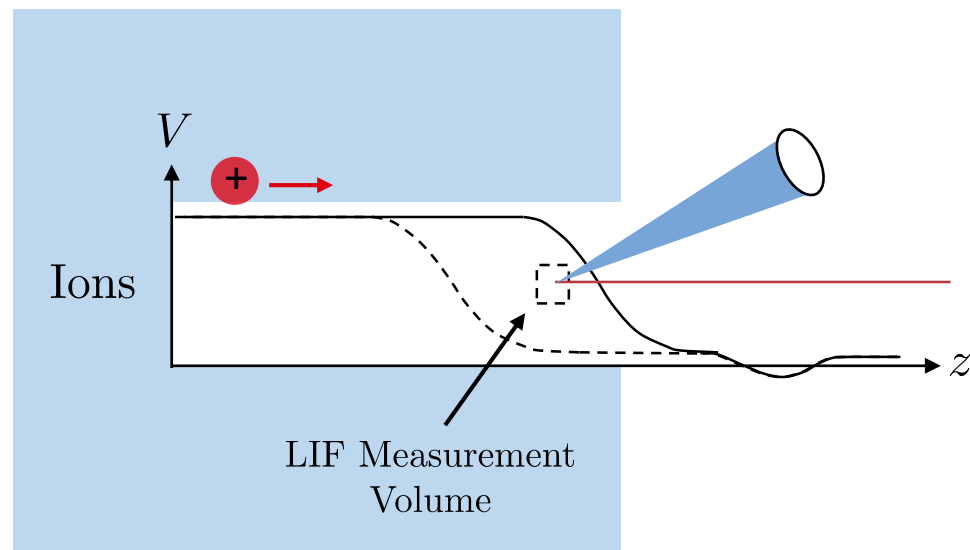
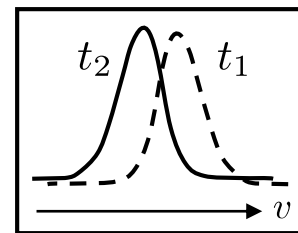
W. Hargus, N. McDonald, C. Charles

Princeton Workshop 2018

Time-Resolved LIF



Time-Resolved LIF: process only part of PMT signal to obtain one velocity measurement *at one time*



Hardware for Time Resolution

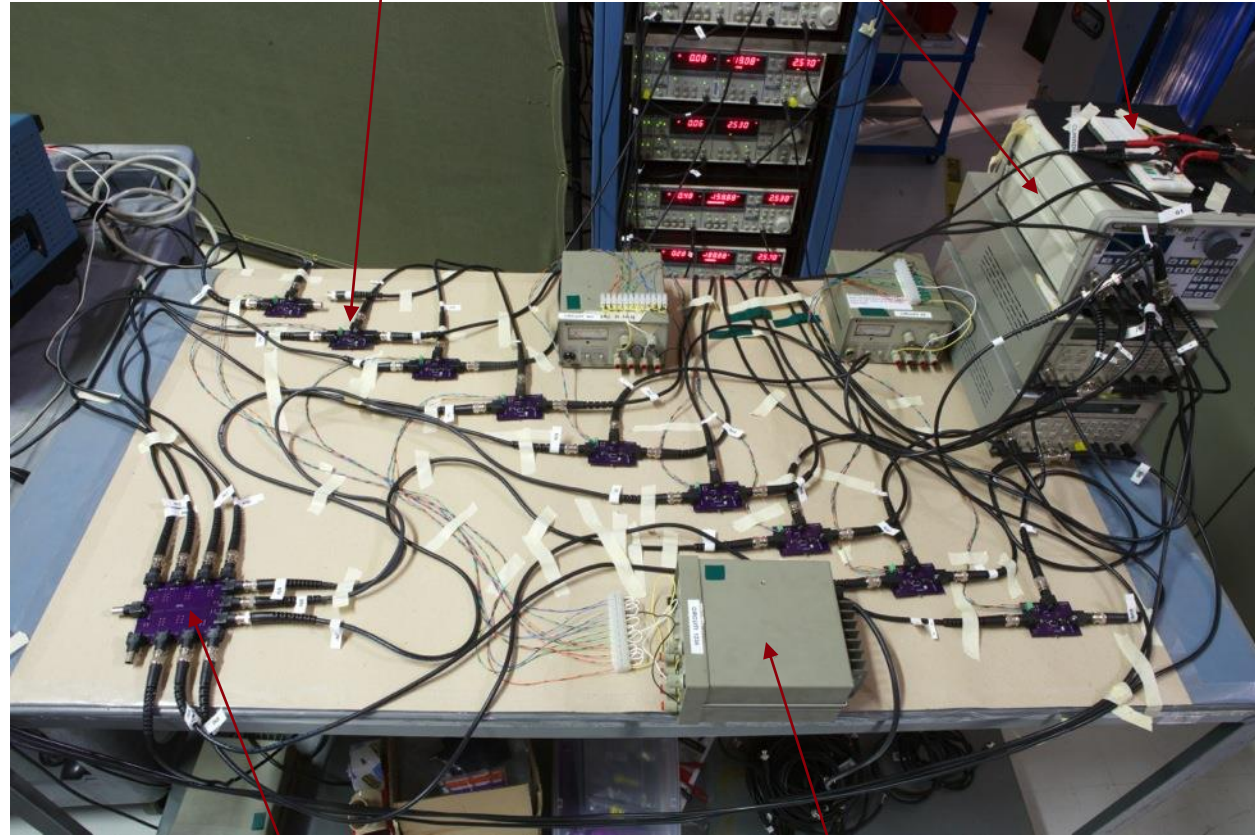


10x SRS Lock-In Amplifiers

9x Sample Hold Circuits

Digital Pulse Delay Generators

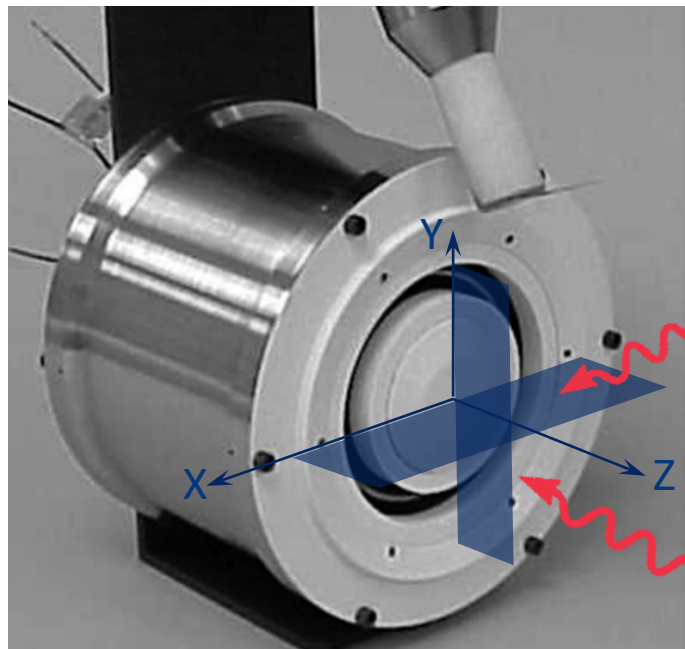
Voltage Comparator



PMT (Voltage) Signal Splitter

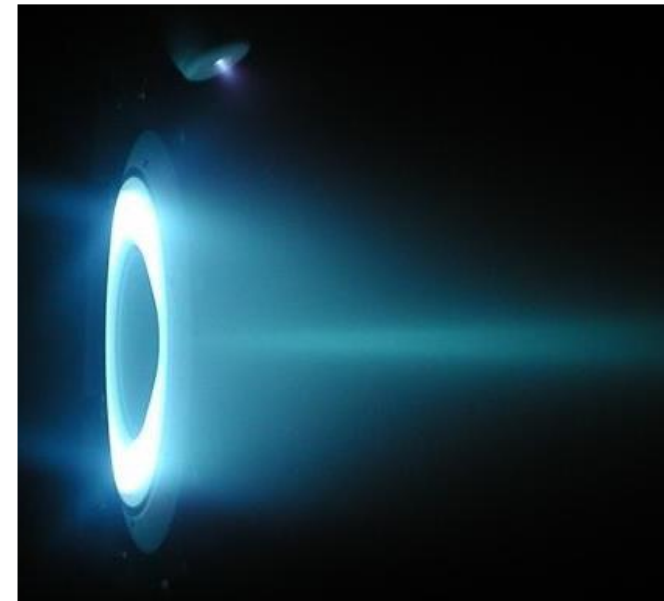
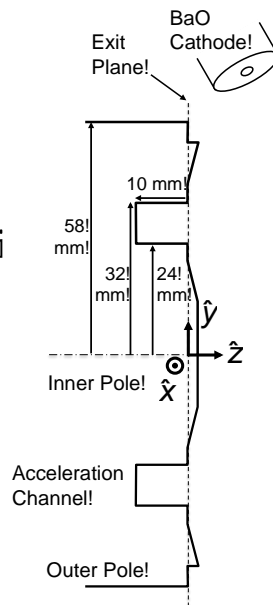
Circuit Power Supplies

BHT-600: Time-Resolved Axial + Radial LIF



Radial

Axial



- LIF measures velocity in direction of beam so 2 beams = 2 velocity components (2D)
- First study of 2-D ion dynamics with time-resolved LIF and largest survey of a single operating condition

■ By the numbers:

Lock-Ins: 10

Scans/Point: 3

Time points: 28

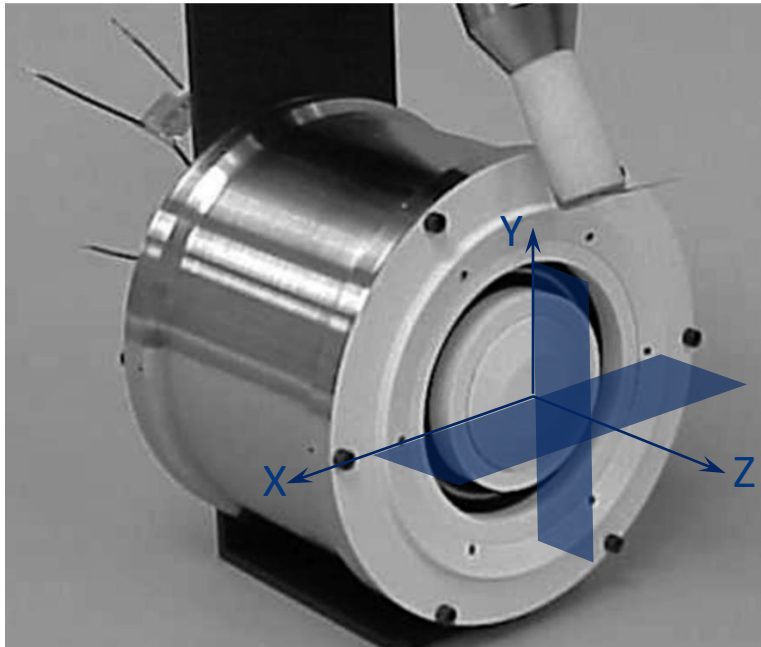
Time Resolution: $1 \mu\text{s}$

Spatial Points: 227

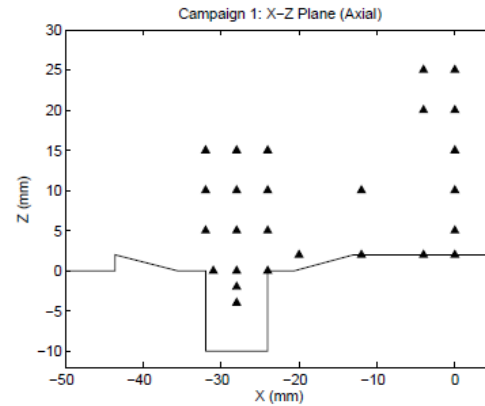
Total Scans: 6356

#VDFs

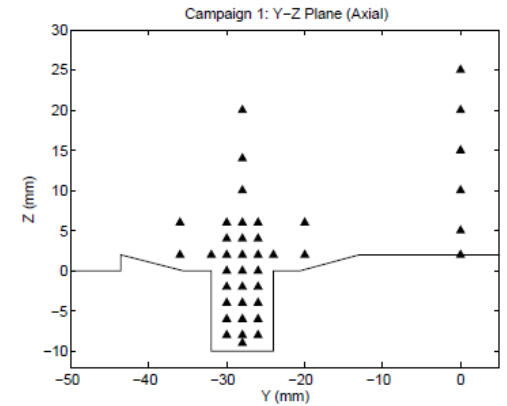
BHT-600 Hall Thruster



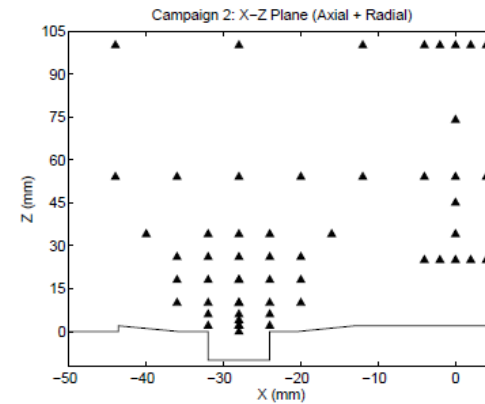
Cathode Bisector



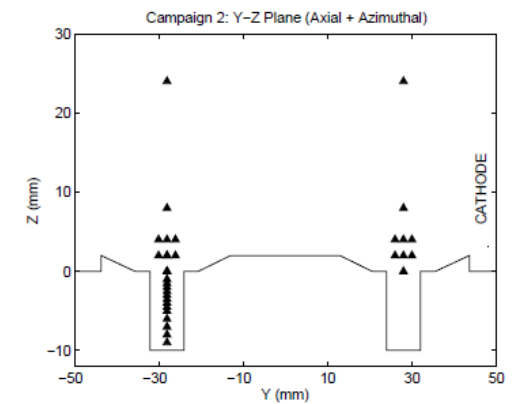
(a)



(b)



(c)



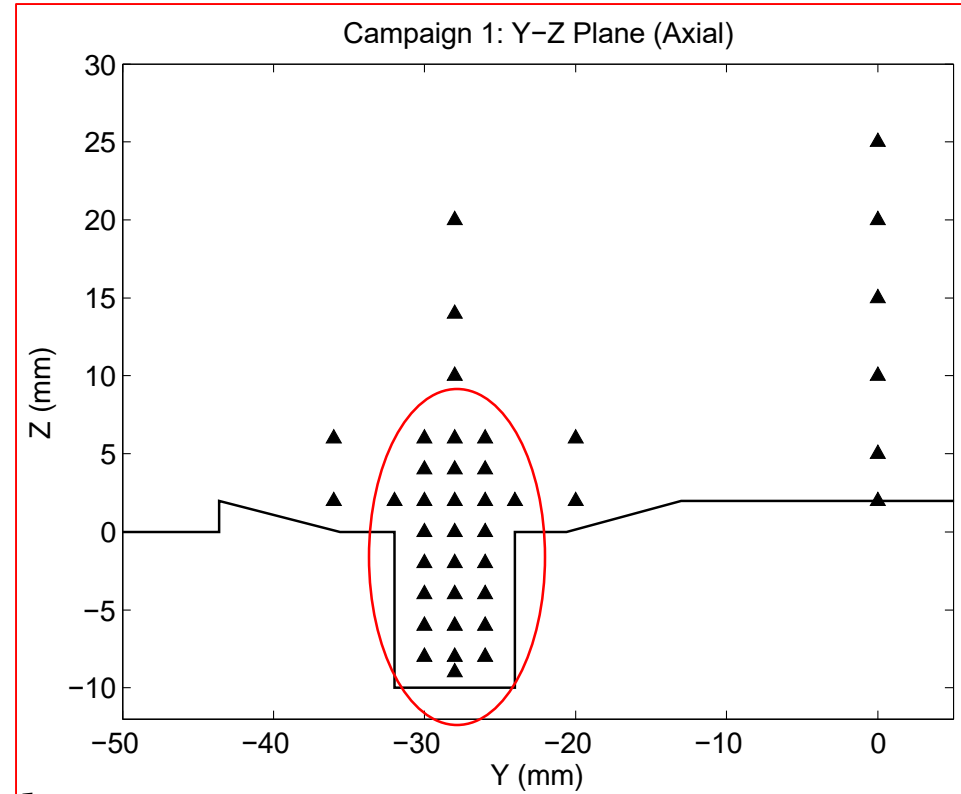
(d)

- Time-resolved axial + radial ion LIF in the plume

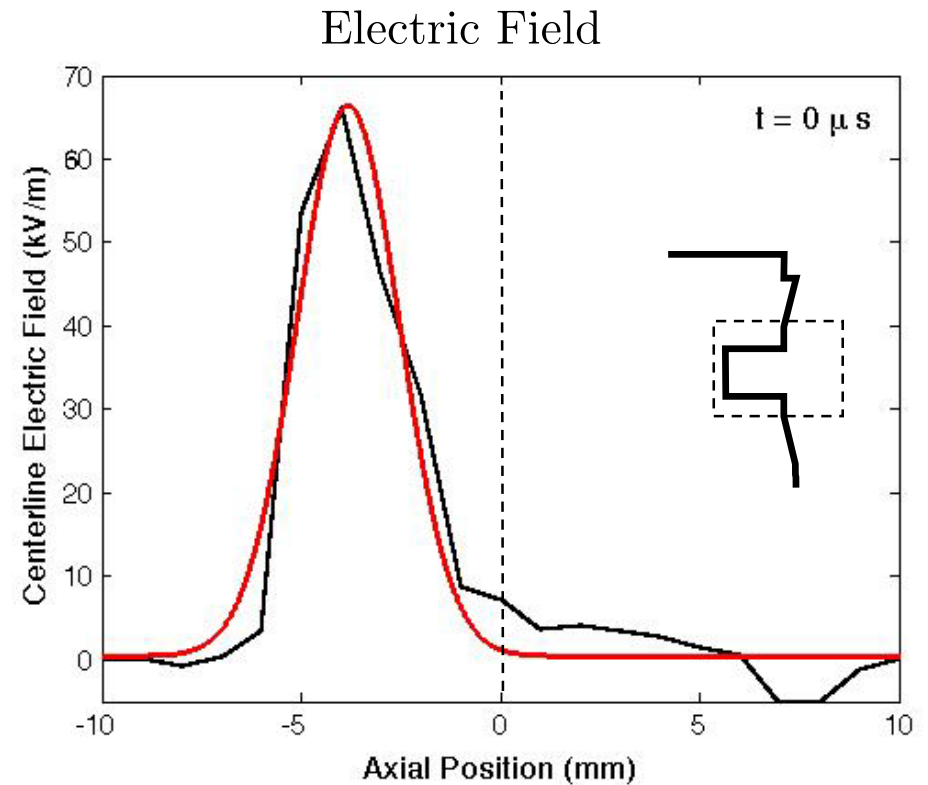
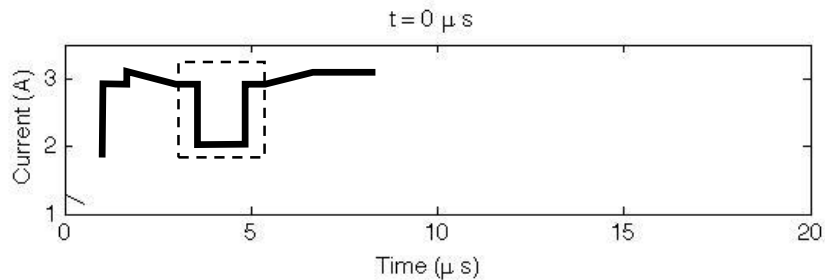
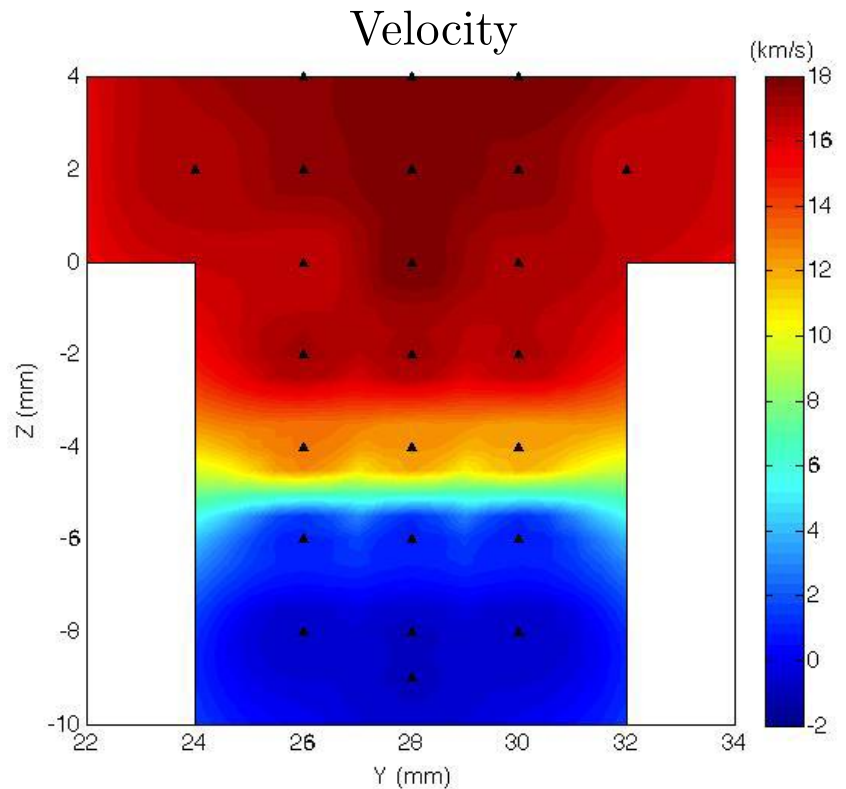
BHT-600 LIF Results: Channel Ion Velocities



Axial



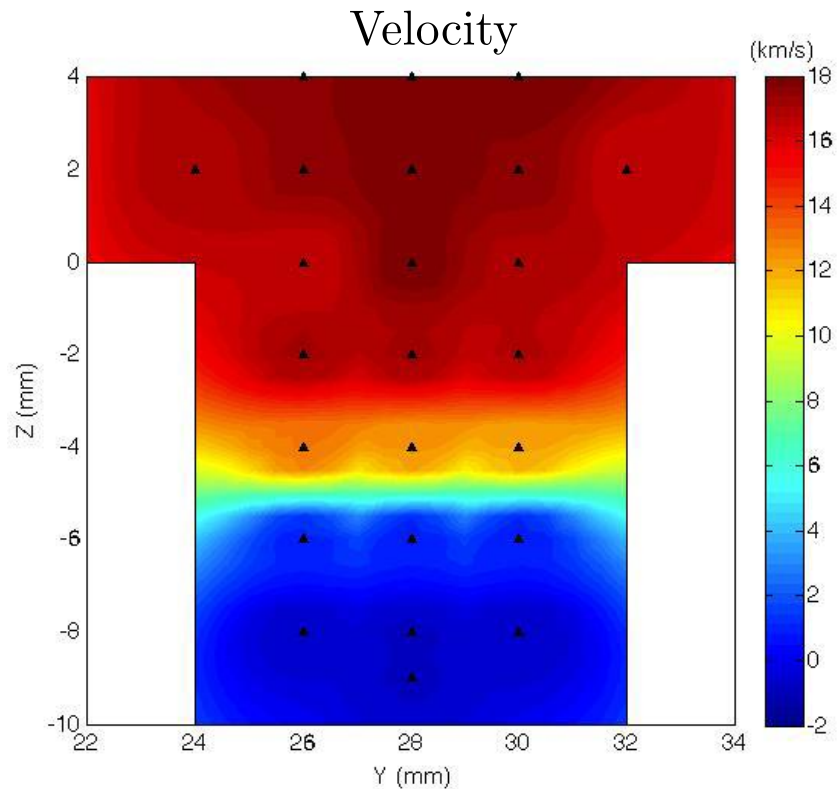
BHT-600 Results: Time-Resolved Channel



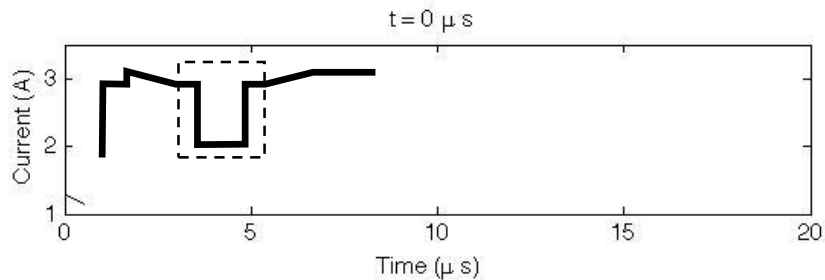
$$E_z = \frac{m_i}{e} \left(\frac{\partial v_z}{\partial t} + v_z \cdot \frac{\partial v_z}{\partial z} \right)$$

- Moving potential hill captured with LIF

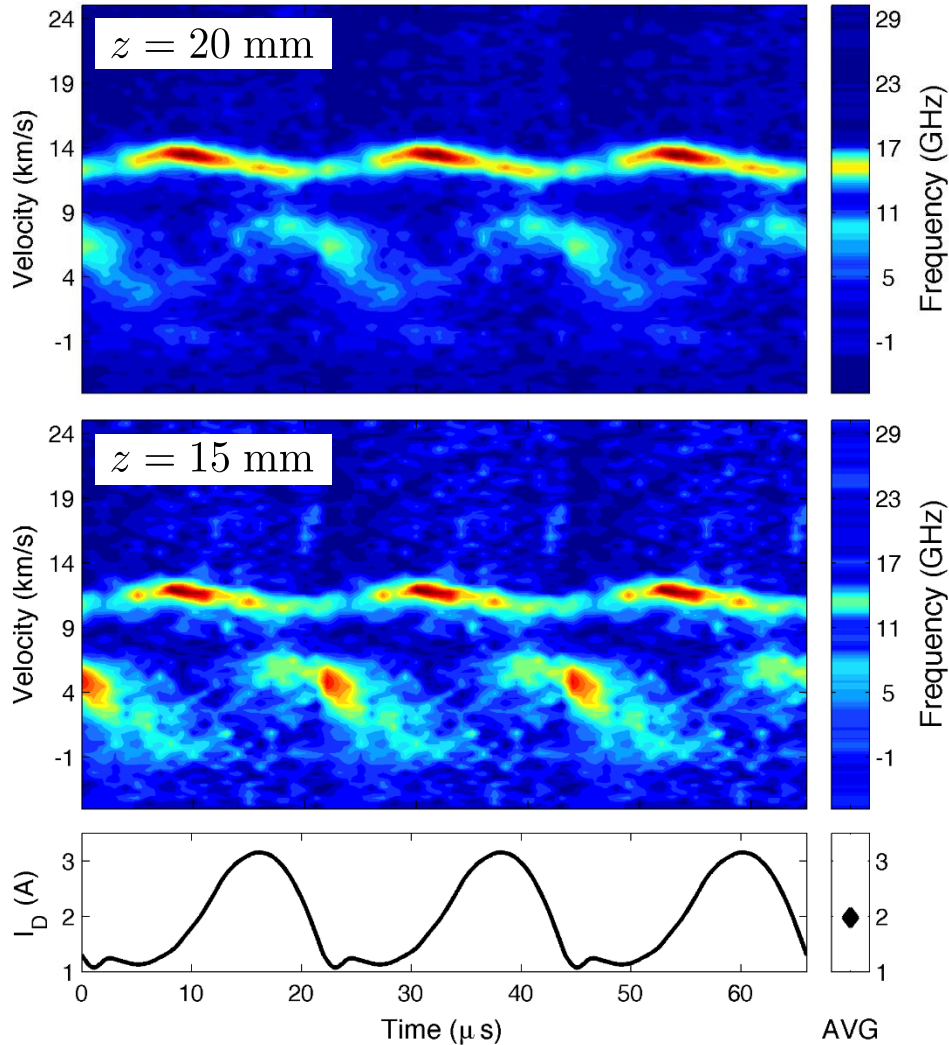
BHT-600 Results: Time-Resolved Channel



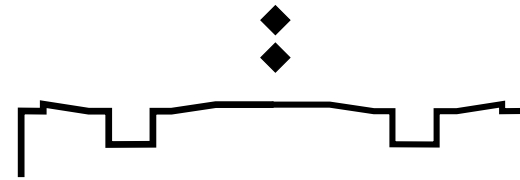
- It seems that the acceleration zone retreats towards the anode when the discharge current decreases



BHT-600 Results: Center Jet, Near Wall



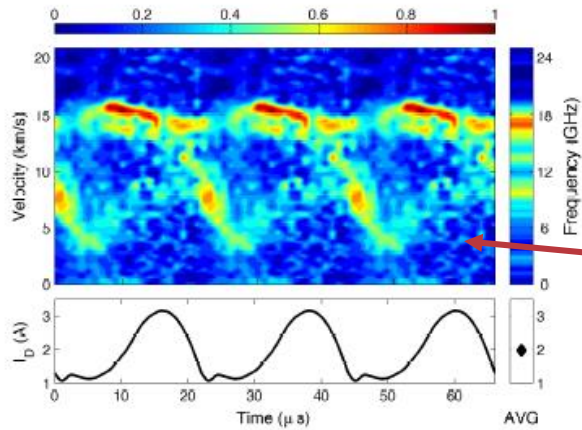
- Axial LIF traces show double populations near the thruster
- Suggests residual ionization is occurring in the central jet with local potential tied to breathing mode dynamics of channel



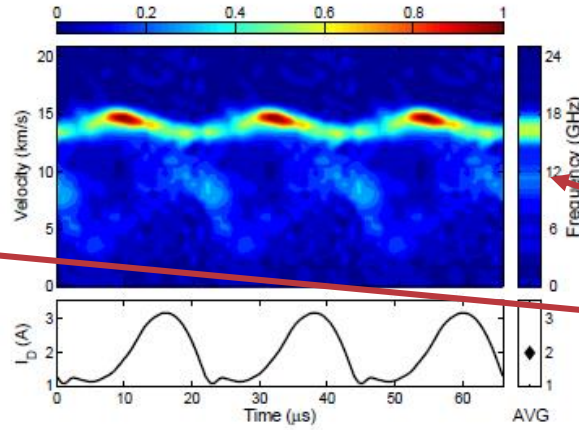
BHT-600 Results: Center Jet, Downstream

Slightly off-centerline

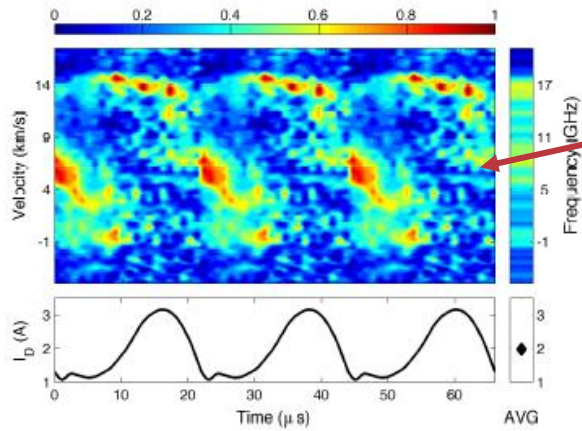
centerline



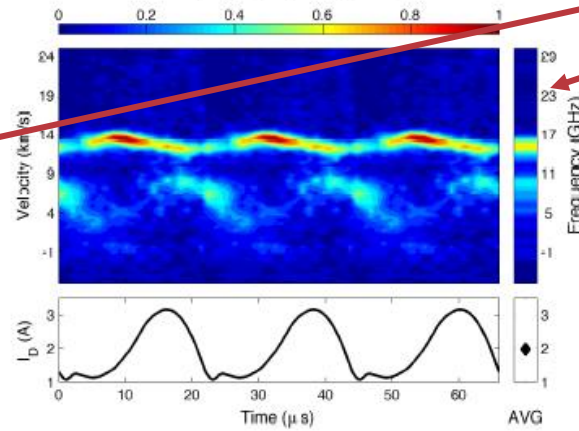
(a) $(x, z) = (-4, 25)$



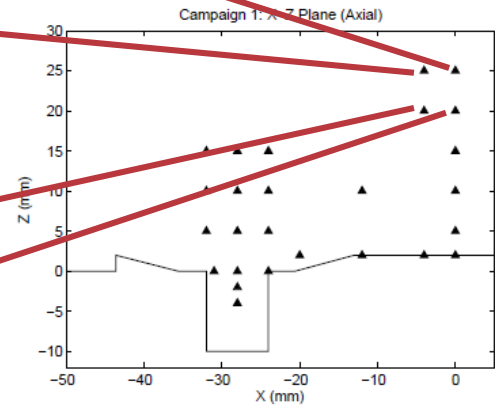
(b) $(x, z) = (0, 25)$



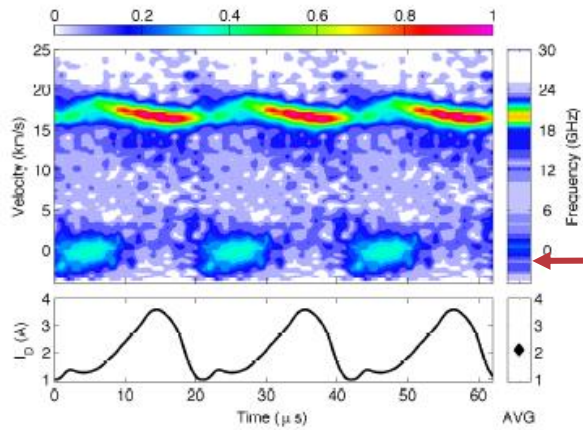
(c) $(x, z) = (-4, 20)$



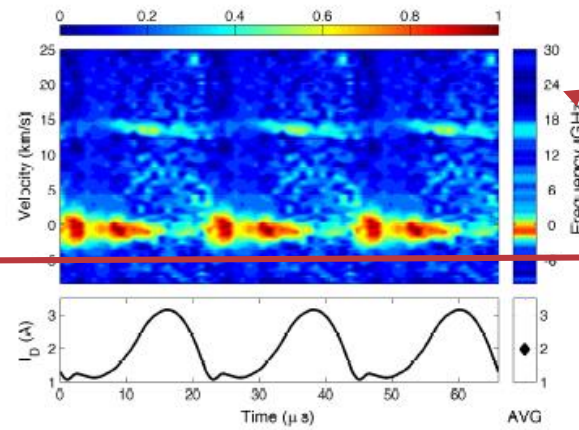
(d) $(x, z) = (0, 20)$



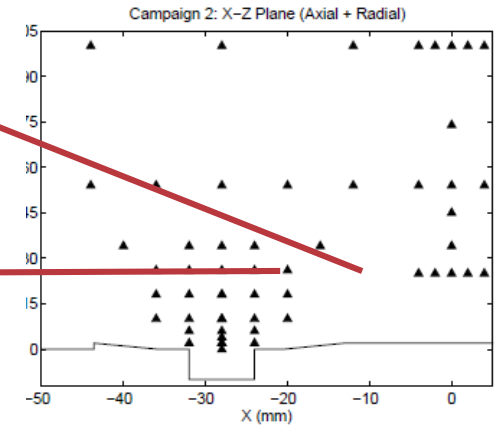
BHT-600 Results: Channel Outside



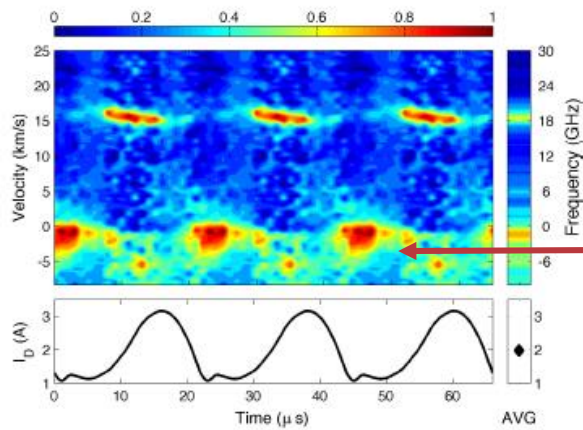
(a) $(x, z) = (-20, 10)$



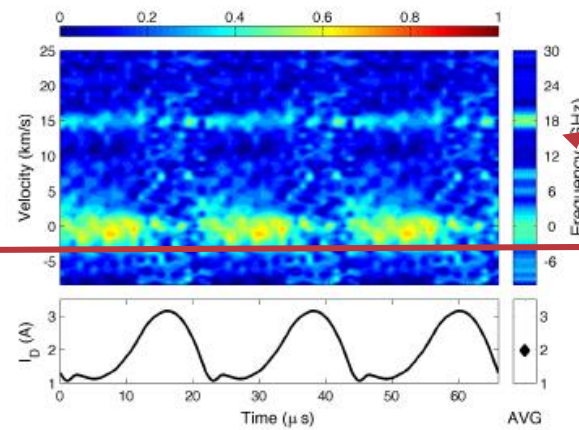
(b) $(x, z) = (-12, 10)$



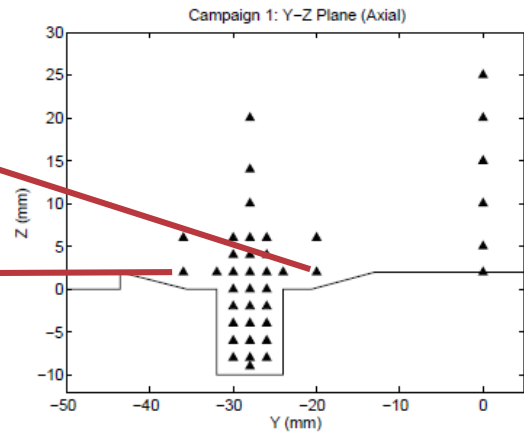
(c)



(c) $(y, z) = (-36, 2)$



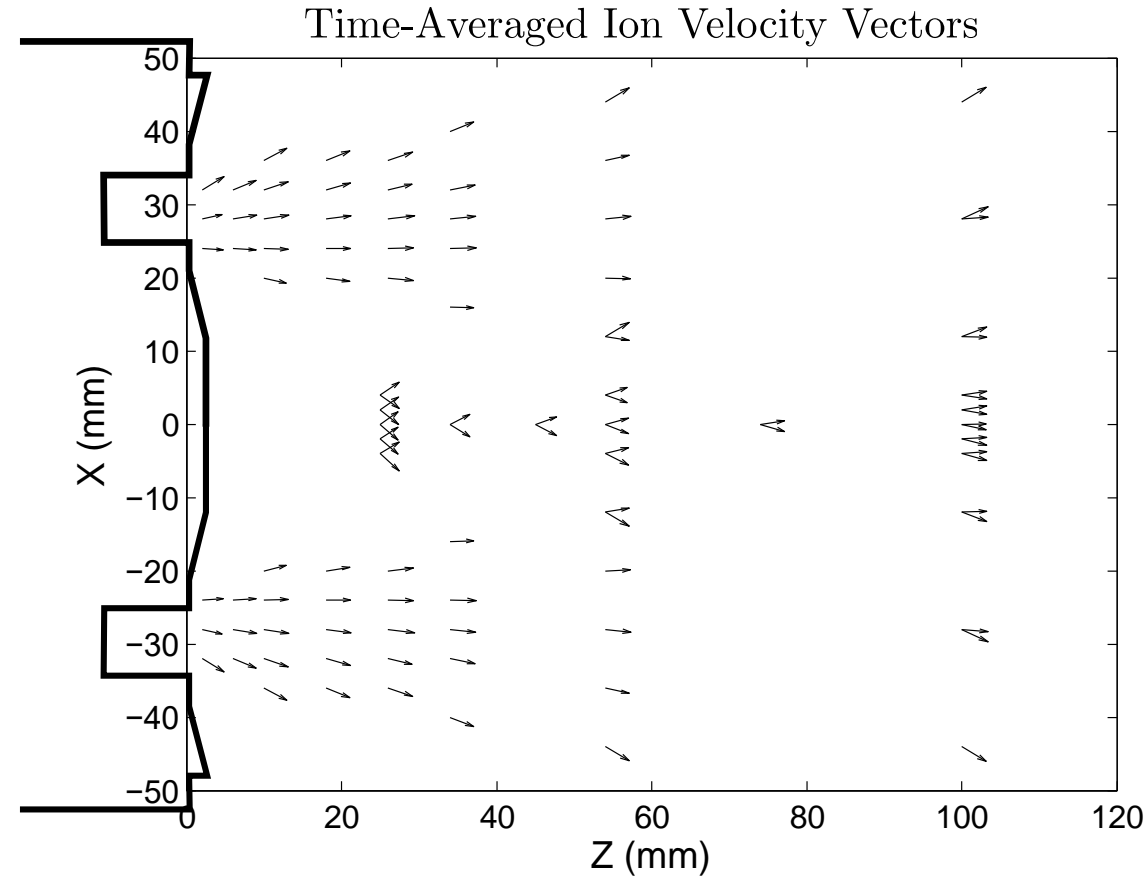
(d) $(y, z) = (-20, 2)$



Thank You

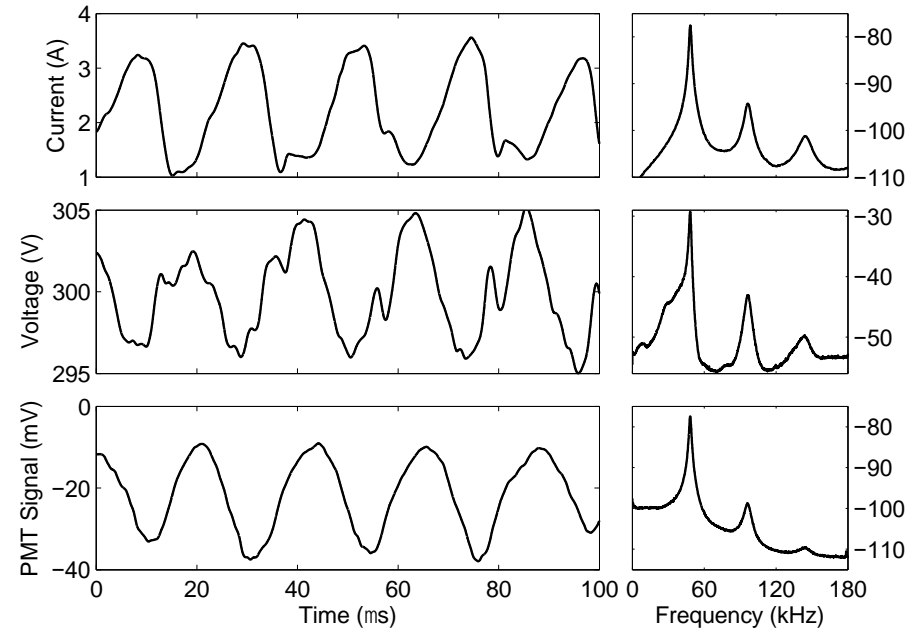
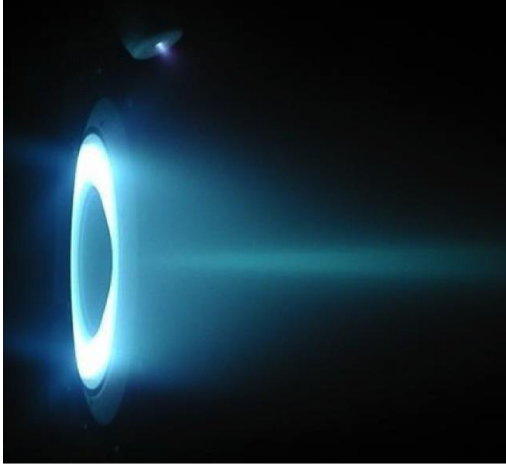
BACKUP
SLIDES

BHT-600 Results: 2-D Plume Ion Velocities



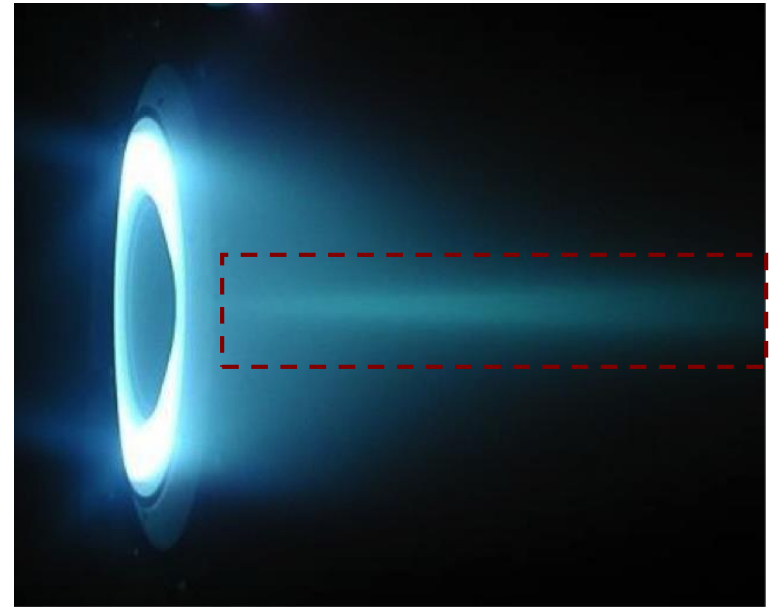
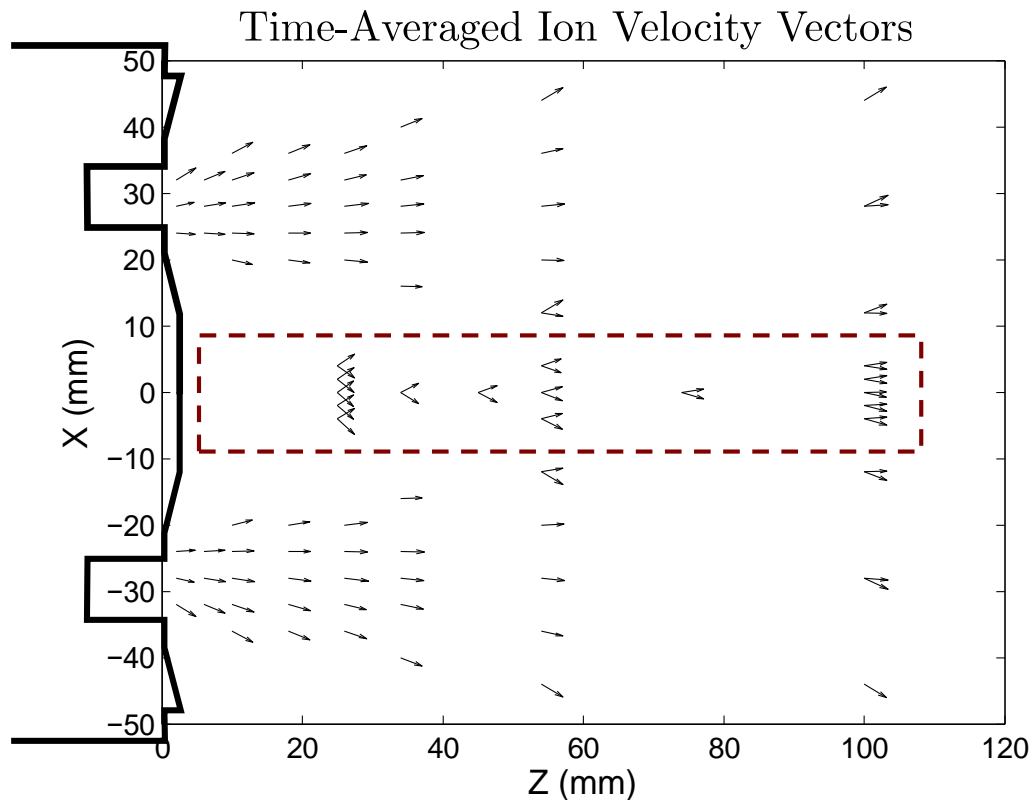
- Time-resolved axial + radial ion LIF in the plume

Hall Thrusters: Breathing Mode



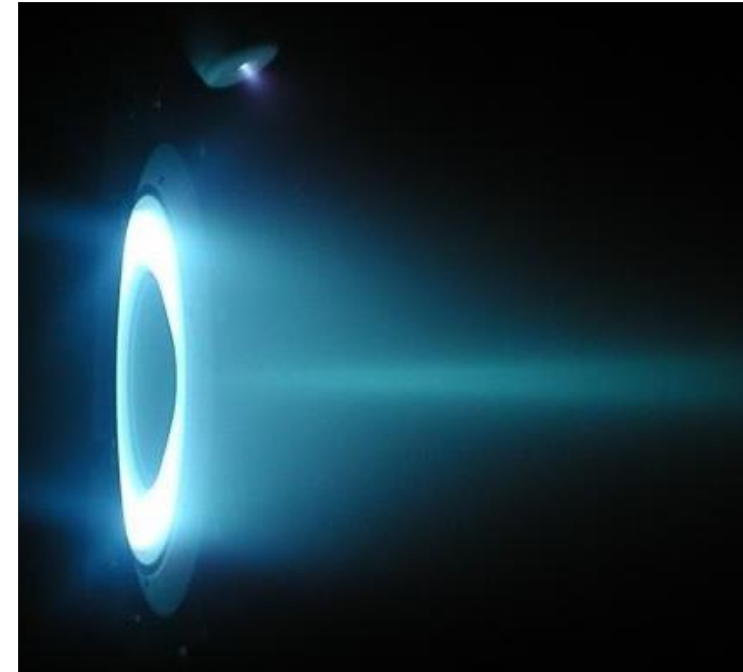
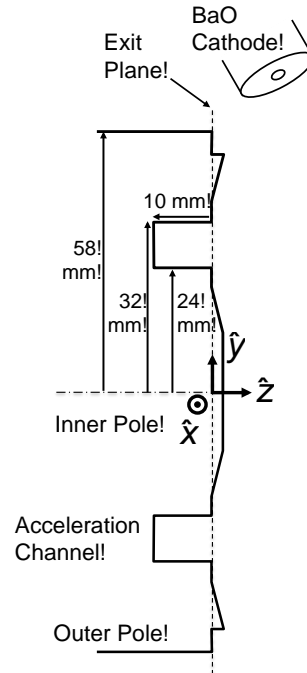
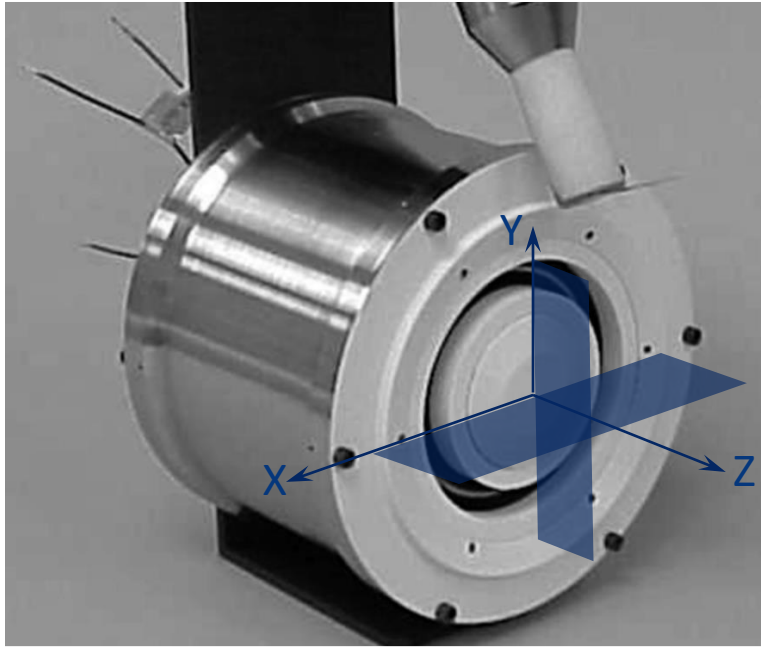
- Thruster works most efficiently when propellant is ionized in cycles
 - Neutrals fill channel
 - Ionization wave moves from exit to anode
 - Ions leave all at once
 - Wait for more neutrals to refill

BHT-600 Results: Center Jet



- Luminous central jet is not well understood and usually appears in efficient operating modes

BHT-600 Hall Thruster



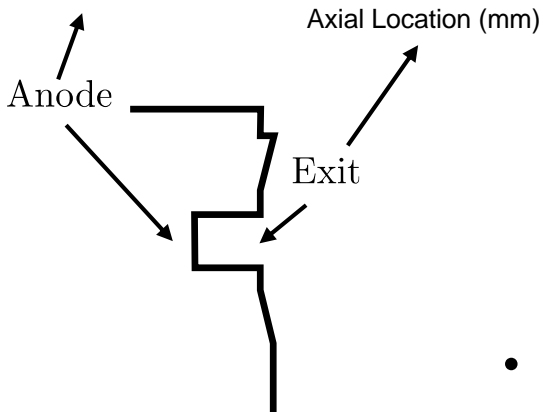
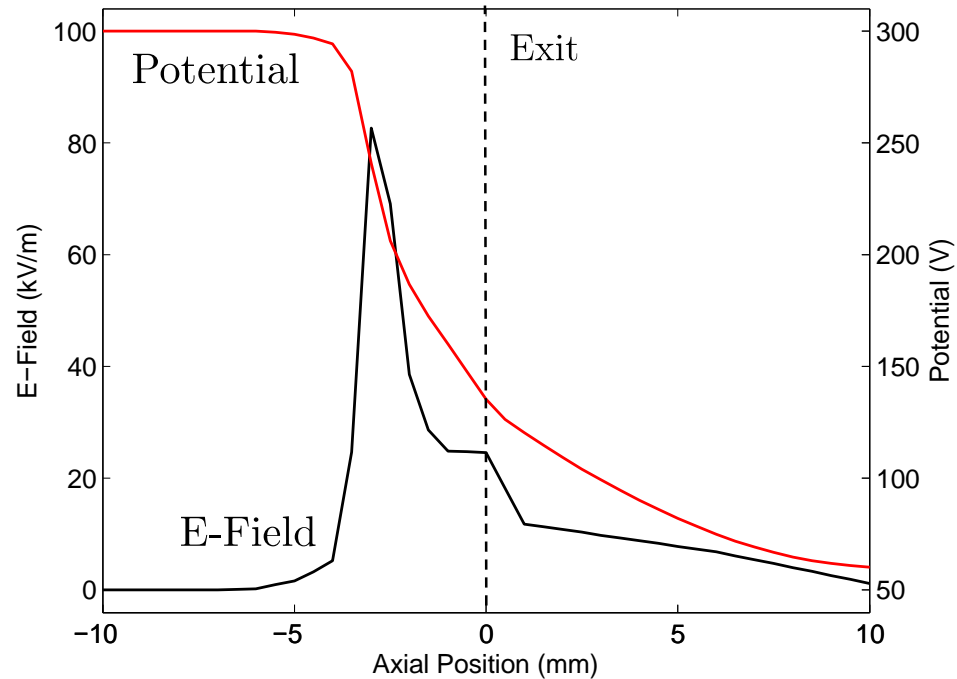
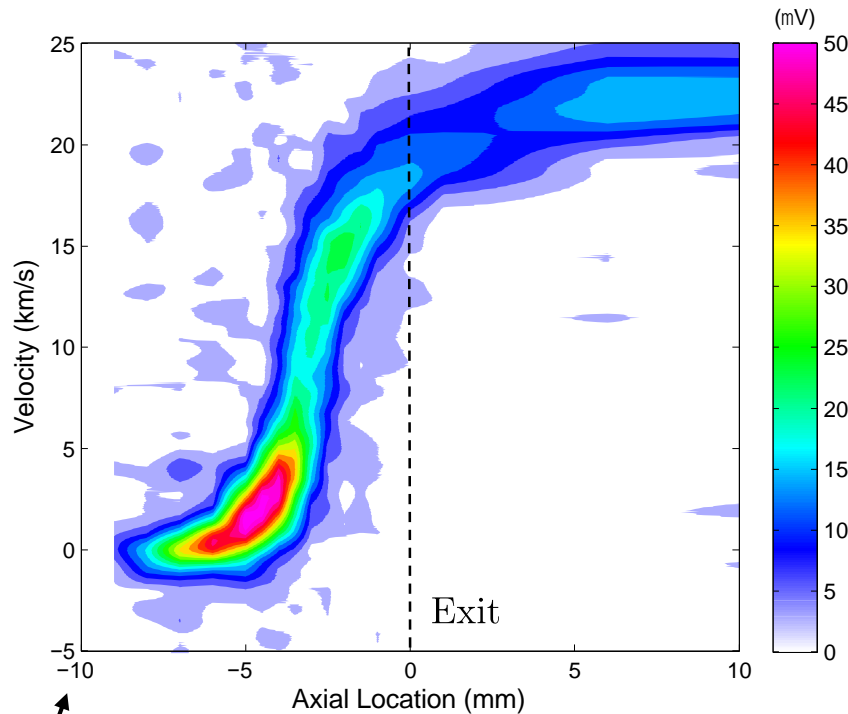
Anode Flow Rate: 2.21 mg/s Xe
Cathode Flow Rate: 147 μ g/s Xe

Anode Voltage: 300 V
Anode Current: 2.05-2.15 A
Anode Power: 630 W

Channel ID: 24 mm
Channel OD: 32 mm
Channel Depth: 10 mm

Thrust: 39 mN
Specific Impulse: 1500 s
Anode Efficiency: 49 %

BHT-600 Results: Time-Averaged Channel

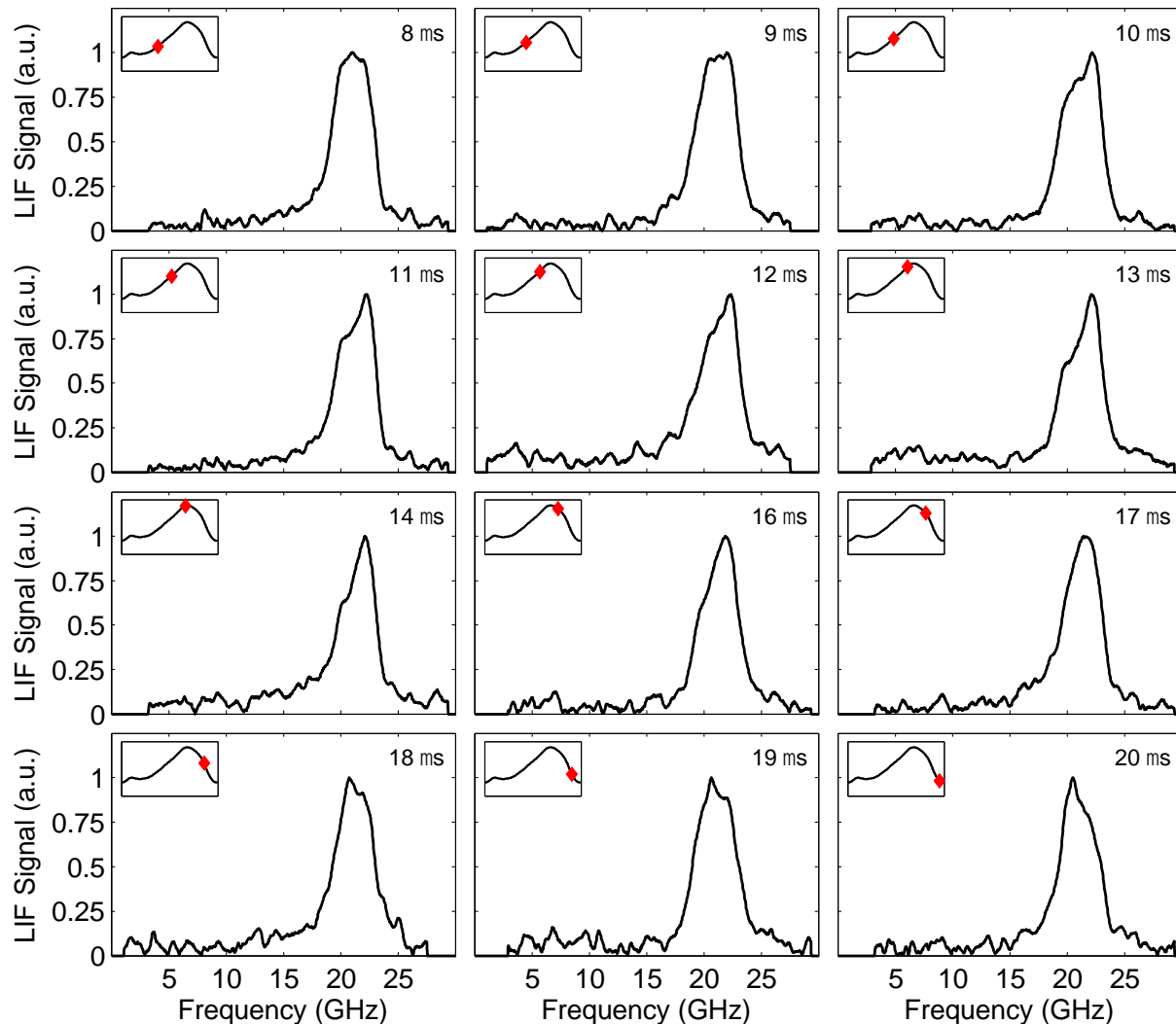


Electric Field:
$$E_z = \frac{m_i}{e} \langle v_z \rangle \frac{d\langle v_z \rangle}{dz}$$

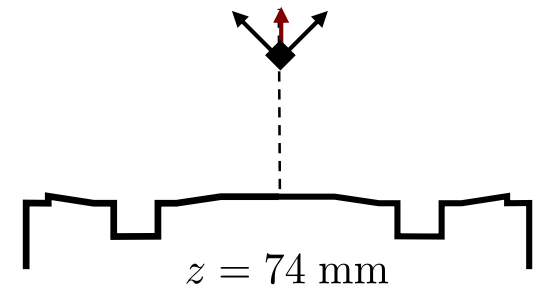
Electric Potential:
$$\phi(z) = \phi_A - \int_{z_A}^z E_z(\bar{z}) d\bar{z}$$

- As usual, time-averaged data only tells part of the story...

BHT-600 Results: Center Jet, Time-Resolved

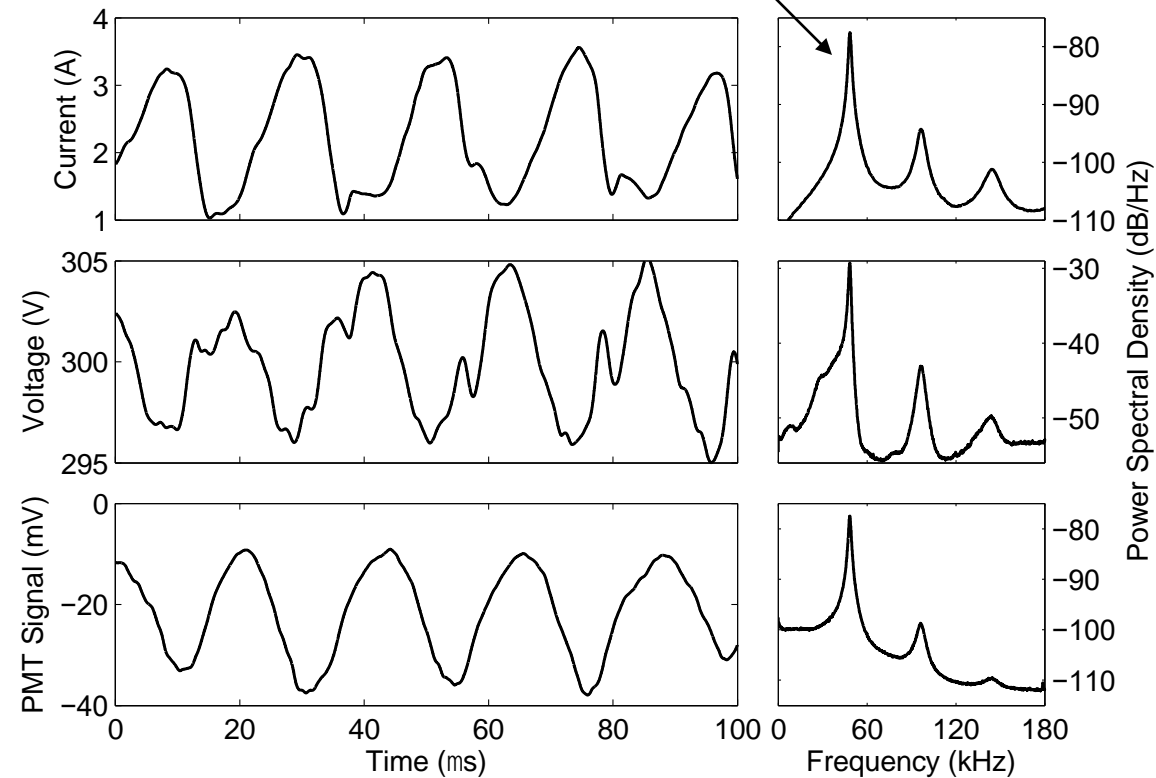


- Axial LIF traces show asymmetry in time:
 - Ion beam from one side of channel dominates for half cycle before switching
- Could be related to helical plasma wave seen previously in plume¹

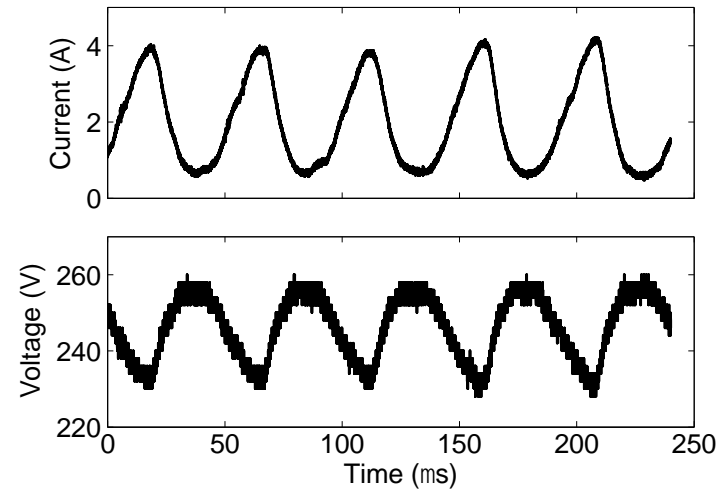


BHT-600 Hall Thruster

Breathing Mode: 43–50 kHz



BHT-600

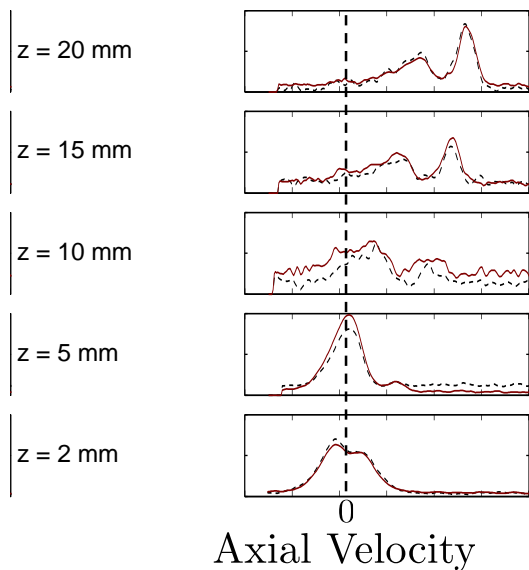
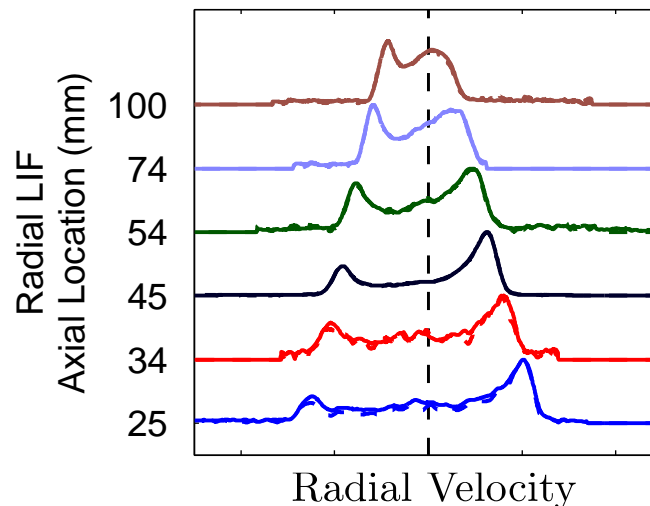
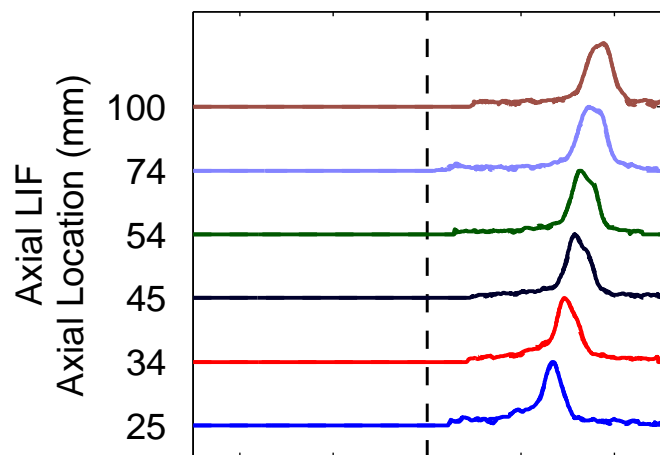


Z-70

- Current and voltage oscillations 180° out of phase in *both* thrusters
- Issue of power supply dynamics influencing thruster operation deserves more attention¹

¹W. Liqiu, et al. *Physics of Plasmas*, **18**, 063508 (2011).

BHT-600 Results: Center Jet, Time-Avg



- Double radial peaks = crossing beams
- Time-averaged radial ion LIF traces are asymmetric – small potential deviations
- Multiple axial ion populations observed closer to the thruster

BHT-600 Results: Particle Visualization

